



HAL
open science

Speciation studies at the Illite - solution interface: Part 2 – Co-sorption of uranyl and phosphate ions

Shang Yao Guo, Mirella Del Nero, Olivier Courson, Sylvia Meyer-Georg, Remi Barillon

► To cite this version:

Shang Yao Guo, Mirella Del Nero, Olivier Courson, Sylvia Meyer-Georg, Remi Barillon. Speciation studies at the Illite - solution interface: Part 2 – Co-sorption of uranyl and phosphate ions. *Colloids and Surfaces A: Physicochemical and Engineering Aspects*, 2024, 684, pp.133129. 10.1016/j.colsurfa.2023.133129 . hal-04489579

HAL Id: hal-04489579

<https://hal.science/hal-04489579v1>

Submitted on 7 Oct 2024

HAL is a multi-disciplinary open access archive for the deposit and dissemination of scientific research documents, whether they are published or not. The documents may come from teaching and research institutions in France or abroad, or from public or private research centers.

L'archive ouverte pluridisciplinaire **HAL**, est destinée au dépôt et à la diffusion de documents scientifiques de niveau recherche, publiés ou non, émanant des établissements d'enseignement et de recherche français ou étrangers, des laboratoires publics ou privés.

1 **Speciation studies at the Illite - solution interface: Part 2 – Co-sorption of**
2 **uranyl and phosphate ions**

3

4 Shang Yao Guo, Mirella Del Nero, Olivier Courson, Sylvia Meyer-Georg, Remi Barillon

5 Institut Pluridisciplinaire Hubert Curien, UMR 7178 Université de Strasbourg/CNRS - IPHC,

6 23 rue du Loess 67037 Strasbourg, France

7

8 *Corresponding author. E-mail address: mireille.delnero@iphc.cnrs.fr - Phone: +33 03 88 10
9 64 08

10 **Abstract**

11 Although it is well known that clays and phosphate ions (hereafter referred to as “P”) can
12 contribute to the long term uptake of uranium (U) in a variety of geochemical systems, work is
13 still needed to document the surface speciation of U(VI) and P sorbed on relevant clay minerals
14 such as illite. Following on from previous work showing strong sorption of phosphate ligands
15 on the surface of a homoionic Na-illite ([1]), we addressed the (competitive/synergistic)
16 mechanisms of (co)sorption of trace levels of uranyl ions (1-10 μ M) and phosphate ligands (100
17 μ M) onto this clay, and the identity of the surface species formed, by in situ spectroscopy
18 monitoring of the clay-solution interface along sorption. We also performed complementary
19 batch sorption experiments and electrophoretic mobility (EM) measurements. Macroscopic
20 data indicated a uranyl sorption dependent on pH, aqueous U concentration and clay-to-solution
21 ratio, a signature of P on the U sorption, and a promotion of P sorption with U concentration.
22 Macroscopic and EM data also suggested mostly reversible mechanisms of P and U co-sorption
23 that confer negative charges on the mineral surface and involve several types of uranyl
24 phosphate surface species and/or surface sites present on the clay edges. FTIR interface spectra
25 confirmed that several types of inner sphere uranyl phosphate surface species formed at acidic
26 pH at the illite-solution interface, as a function of U surface coverage and/or reaction time. An
27 inner-sphere uranyl phosphate surface complex, likely with a U-bridging structure, was formed
28 rapidly on high-affinity surface sites existing in limited quantities on the clay edges. Another
29 U-P surface complex (with a possible P-bridging structure) was progressively formed in
30 increasing amounts with U surface coverage and time on low affinity clay edge sites. Finally, a
31 third U-P surface species having an autunite-like structure (probably a U-P polynuclear surface
32 species) was formed on the illite surface at high U concentration (10 μ M). The two later species
33 competed with the existence on the illite surface of inner sphere surface complexes and outer-
34 sphere surface complex of phosphate, which were identified in the absence of U. Information

35 on uranyl surface speciation in the presence of phosphate ligands presented here is novel and
36 provides for the first time in situ spectroscopic evidence of synergistic U-P sorption process
37 leading in the formation of several types of uranyl phosphate sorption species on the surface of
38 illite. These results provide a sound basis for better understanding / prediction of U sorption in
39 the environment, including in clayey formations being considered as long term barriers to
40 radionuclide migration in far field of high level nuclear waste repository.

41

42 **Keywords**

43 Illite, Uranyl sorption, Phosphate ligands, Surface speciation, In-situ ATR FTIR spectroscopy,
44 / Environment.

45

46 **1 Introduction**

47 The environmental behavior of uranium (U) is a major issue of soil - sediment - water continua
48 due to the natural abundance of this metal in rocks, its involvement in a variety of anthropogenic
49 activities such as metal mining, water treatment and energy production [2–4], its radiological
50 and chemical toxicity, and the complexity of the biogeochemical processes that govern its fate
51 in ecosystems [5,6]. Nuclear power plants generate spent nuclear fuel containing U and produce
52 radioactive wastes, for which various long-term management strategies have been proposed
53 including the disposal of high-level radioactive wastes (HLW) in repositories in deep geological
54 formations [7–9]. Near field engineered barrier systems will isolate stored HLW from
55 groundwater and prevent dissolution, but their progressive degradation poses a long term safety
56 issue. Hence, to prevent migration of dissolved and colloidal radionuclides (RN) in
57 groundwater –as a result of long term HLW dissolution- into the human-accessible environment,
58 host argillaceous rocks as geological far-field barriers, such as Callovo-Oxfordian clay, COX,

59 and Opalinus clay, OPA [10], have been considered by several countries. These rocks have clay
60 minerals as their main constituents and outstanding physicochemical properties for storage,
61 such as low permeability and high mineral retention capacity for RN, including U ([11–16]).
62 Uranium -which exists mainly in environment in the IV and VI oxidation states- is indeed
63 known to be potentially mobile in the hexavalent state as uranyl ions, UO_2^{2+} [5], which
64 participate in formation of a variety of aqueous complexes given the high chemical affinity of
65 U(VI) for the dissolved ligands OH^- and CO_3^{2-} [17–20], organic ligands [6,21] and phosphate
66 ligands, PO_4^{3-} (hereafter referred to as “P”) [22,23]. In particular, phosphate ligands can
67 promote U(VI) retention in rocks or soils via precipitation and / or sorption processes.
68 Precipitation of U(VI) phosphates like chernikovite or autunite can limit U solubility under
69 certain conditions [22,24–28]. Moreover, secondary uranyl phosphate precipitates were found
70 in the vicinity of U-ore deposits or in contaminated sediments [24,29–38] and U was shown to
71 exist in close association with P and iron(III)/Al(III) oxihydroxides or clays [32,34,39–44] in
72 some soils or surface environments. Due to the ubiquity of phosphate minerals/ligands in clay
73 rock-soil-water continua, a thorough understanding of the mechanisms of U(VI) and P(V) co-
74 sorption on relevant minerals is mandatory to provide a solid basis on which to build a robust
75 assessment of the fate of uranium in the environment.

76 The objective of this work is to provide new insights into the mechanisms and surface species
77 involved in uranyl and phosphate ions co-sorption onto illite, a main constituent of clay rocks
78 including COX. Numerous studies have reported strong sorption of uranyl ions at surfaces of
79 metal oxihydroxides [45–48] and clay minerals / rocks [11,13,15,49–53], and the promoting
80 effect of P sorption on retention of U(VI) on metal oxihydroxides and kaolinite, at acidic/neutral
81 pH [45,46,54–56]. In addition, spectroscopic studies have clarified the surface speciation of
82 U(VI) sorbed to Al and Fe oxihydroxides [57–63] and clays [13,53,64–68], in the absence of P.
83 However, far less spectroscopic work has been devoted to mineral-solution systems containing

84 uranyl and phosphate ions (or arsenate ions as P homologues) and little structural data exist on
85 the U and/or P surface species formed [55,68–70], particularly on clays [71,72]. Troyer et al.
86 [71] have reported no significant P sorption (in absence of U) on montmorillonite and no P
87 signature on the sorption of U, which was controlled by formation of inner-sphere surface
88 complexes (ISSC) of uranyl phosphate (with U-bridging). Further work is required to identify
89 the U/P species formed on the surface of clays like illite and kaolinite, for which a strong P
90 sorption and/or signature on U sorption has been reported, and thus clarify the effect of clay
91 surface properties.

92 Spectroscopic studies have evidenced that, in the absence of P, U(VI) sorption species existing
93 on Fe(III) oxi-hydroxides are surface-U(VI)-carbonato complexes formed in a wide pH range
94 [57,58] and bidentate ISSC of U(VI) on goethite [69]. For Al oxihydroxides, formation of the
95 former has also been reported, notably under conditions where uranyl tricarbonato species exist
96 in solution [63], and effect of U loading has been demonstrated on the main forms of sorbed
97 U(VI) (bidentate ISSC vs polynuclear surface species of U(VI) [60,61]; or surface carbonato
98 complex vs. oligomeric surface complex / precipitate of U(VI) [62]). For clays, multiple U(VI)
99 sorption species have also been identified, even at low U concentration (for example, [53]).
100 U(VI) was sorbed as exchangeable UO_2^{2+} in the montmorillonite interlayer space, in addition
101 to uranyl ISSC and/or U(VI) polynuclear surface species [13,64–66] and surface-U(VI)-
102 carbonato complexes formed at clay edge sites [67]. In the presence of phosphate ligands, too,
103 spectroscopic studies have concluded that sorbate surface coverage and pH are main parameters
104 controlling U(VI) surface speciation. Based on Extended X-Ray Absorption Fine Structure
105 (EXAFS) spectroscopic studies, Singh et al. [59] have evidenced U sorption onto goethite via
106 formation of U-phosphate-Fe(III) oxide surface complexes, at acidic / neutral pH, and low and
107 moderate concentrations of U ($\leq 10\mu\text{M}$) and P ($100\mu\text{M}$). These authors have indicated a U-
108 bridging structure for the surface complex but have suggested that the presence of a P-bridging

109 structure was statistically possible. Studies using in situ Attenuated Total Reflection Fourier
110 Transform Infrared Spectroscopy (ATR FTIR) and Time Resolved Laser Induced Fluorescence
111 Spectroscopy (TRLFS) have shown that U(VI) was sorbed at alumina-P-solution interface via
112 the formation of uranyl phosphate ISSC, with a gradual transition to surface precipitation of
113 U(VI)-phosphate with increasing P loading [55,70]. To our knowledge, only two spectroscopic
114 studies have been devoted to the co-sorption of uranyl and phosphate ions on clay surfaces.
115 Gładys-Plaska et al.[72] have pointed out, on the basis of X-ray Photoelectron Spectroscopy
116 (XPS) and ATR FTIR data, that two types U(VI)-phosphate surface complexes, those with a
117 high and those with a low P content in their structure, are formed on the edge sites of red clays
118 during simultaneous sorption of U(VI) and phosphate ions. Troyer et al. [71] have used EXAFS
119 and TRLFS to investigate the effect of P and U concentrations on U(VI) surface speciation on
120 montmorillonite, and have evidenced a transition between formation of surface complex and
121 surface precipitates of U(VI)-phosphate with increasing sorbate surface coverage at pH 4-6, as
122 well as existence of a uranyl carbonate surface complex at pH 8. The authors have indicated a
123 U-bridging structure for the ternary surface complex, which was most consistent with their
124 macroscopic data. In contrast to montmorillonite, P was found to exhibit a significant
125 macroscopic sorption on Na-illite ([1]) and in situ ATR FTIR spectroscopic evidence has been
126 given that P was sorbed via formation of phosphate ISSC at edge sites of illite platelets. The
127 question arises as to the mechanisms of U-P (co)sorption in such a system, namely competition
128 between uranyl and phosphate ions for surface binding and/or the formation of U(VI)phosphate
129 surface species. In situ spectroscopic monitoring of the clay-solution interface during the
130 sorption process is mandatory to answer this question of the (competitive/synergistic)
131 mechanisms, and U/P species identity.

132 The purpose of this study was to identify the mechanisms and (multiple) U-P species involved
133 in the retention of low concentrations of U(VI) on homo-ionic Na-illite, in the presence of

134 phosphate ligands, by in situ ATR FTIR spectroscopic monitoring of the clay - U(VI) -
135 phosphate - solution interface during sorption. In situ ATR FTIR sorption experiments were
136 carried out to record FTIR spectra of the interface as a function of parameters like reaction time
137 and U surface coverage (total U concentrations, $[U]_{l,aq}$: 1-10 μ M). Sorption species were
138 identified by (changes in) the coordination environments of the sorbed phosphate units, which
139 were deduced from changes in the FTIR interface spectra recorded in the 900-1200 cm^{-1} region
140 (characteristic of P-O stretching vibrations), and comparison with FTIR phosphate sorption data
141 previously acquired in the absence of U ([1]). In complement, batch sorption experiments were
142 carried out to quantify the macroscopic retention of U and P as a function of pH (sorption edges)
143 at different clay/solution ratios ($R_{s/L}$: 1-3 $\text{g}\cdot\text{L}^{-1}$). Sorption isotherms were determined at acidic
144 pH over a range of total U ($[U]_{l,aq}$: 1 – 25 μ M) and P ($[P]_{l,aq}$: 20 – 200 μ M) concentrations.
145 Electrophoretic mobility (EM) measurements of suspended clay particles were also carried out
146 to determine the sign of charges imparted to the illite surface by sorption reactions. This study
147 presents the first published in situ surface speciation of uranyl and phosphate ions sorbed in
148 illite – U(VI) – P(V) - solution systems. Mechanistic data given here on competitive /
149 synergistic sorption of U and P on illite is central to improve our knowledge on the retardation
150 mechanisms of U(VI) by clay formations such as those envisioned as far-field host rocks in
151 HLW repository.

152 **2 Materials and methods**

153 Analytical grade chemical products and ultrapure Milli-Q water (purity >18 $\text{M}\Omega\cdot\text{cm}$) were used
154 in all experiments.

155 *2.1 The clay sample used*

156 The clay sample used is a homoionic Na-Illite (noted as NaIdP) obtained by conditioning of a
157 size fraction (< 77 μm) of Illite du Puy (referred “IdP”) purchased at a company (Argile Verte

158 du Velay of Lissieu) and collected in “Le Puy-en-Velay” region in Massif Central Mountains
159 in France. The conditioning procedure [73] allows to remove hydrolyzed products such as
160 hydroxy-aluminium compounds, phosphate impurities and calcite [14,73]. Methods used and
161 mineralogical and chemical characteristics of the samples are detailed in Guo et al. [1] and are
162 summarized hereafter. Specific surface areas of IdP and NaIdP were found to be equal to 92
163 and 107 m².g⁻¹, respectively, in agreement with a previously published value of 97 m². g⁻¹ [50].
164 Mineralogical composition of whole rocks and their clay size fractions (< 2 μm), as obtained
165 by X-ray diffraction analyses, layer / interlayer spacings of clays (e.g. Brindley and Brown [74])
166 and semi-quantitative estimates by using the DIFFRAC.EVA software (4.3 version, error <5%)
167 are as follows. IdP is mainly composed by calcite (38%), feldspars (36%) like microcline,
168 orthoclase and albite, and illite (19%) and low amounts of kaolinite, quartz, siderite, and
169 hematite. Main minerals of NaIdP are Na-illite (30%) and feldspars (58%) and accessory
170 minerals are quartz and kaolinite. Clay fraction of both samples only contains illite (> 75%) and
171 kaolinite. Major element composition of NaIdP obtained by Inductively Coupled Plasma
172 Optical Emission Spectrometry analysis (ICP-OES, analytical error <0.1%) is consistent with
173 that of a K-rich silicate rock and with removal of carbonate minerals and phosphate minerals
174 during clay conditioning (CaO < 1% in wt/wt % oxide and P₂O₅ under detection limit). It is to
175 be noted that Fe concentration remains significant (Fe₂O₃: 8% in wt/wt % oxide) and indicates
176 either presence of accessory Fe-minerals (< 5%) and/or an incorporation of Fe in clay structures.
177 Trace metal element (TME) compositions obtained by ICP Mass spectrometry (ICP-MS,
178 analytical error: 5-20 %) indicate that concentrations of Sr, As and Ln are lower in NaIdP than
179 IdP, likely due to removal of carbonate and/or phosphate minerals during clay conditioning.
180 Concentrations of other trace metal elements (TME) are similar in both clay samples (> 150ppm
181 for Rb, Ba, Zn, Cr and Cs; < 50 ppm for other TME; ca. 3 ppm for U).

182 2.2 *Batch sorption experiments*

183 Experiments carried out in the Part 1 of this study ([1]) have provided data on the chemical
184 evolution of a 0.005 M NaCl electrolyte solution brought in contact with (Na)IdP samples.
185 Phosphate ions were main inorganic ligands released in solution during IdP-solution
186 equilibration. Such a release is expected to affect the behavior of uranium (VI) at trace level in
187 Illite du Puy –solution systems. No significant amounts of phosphate ions and uranium(VI)
188 were detected in final experimental solutions equilibrated with NaIdP. This sample was thus
189 chosen to study the (co)sorption processes of uranyl ions and/or phosphate ions onto clay, under
190 well-controlled laboratory conditions.

191 2.2.1 Uranyl sorption

192 Batch experiments were carried out under atmospheric conditions and at 298K to evaluate the
193 effect of pH, total concentration of uranyl ions ($[U]_{I, aq}$) and clay-to-solution ratio ($R_{S/L}$) on the
194 macroscopic uptake of uranyl ions by NaIdP. Sorption edges were obtained at pH 3-8, at
195 different values of $[U]_{I, aq}$ (1 and 12 μM) and $R_{S/L}$ (1, 2 and 3 $\text{g}\cdot\text{L}^{-1}$). Sorption isotherms ($[U]_{I, aq}$
196 varying from 1 to 10 μM) were obtained at pH 3, 3.5 and 4, respectively, and at $R_{S/L}$ equal to 3
197 $\text{g}\cdot\text{L}^{-1}$. The individual experiments were conducted at defined values of $R_{S/L}$ and pH as described
198 below. Defined amounts of NaIdP subsamples were introduced in individual 15 mL
199 polypropylene tubes and brought in contact with an electrolyte solution (10 mL of 0.005 M
200 NaCl), at defined initial pH value. The suspensions were pre-equilibrated during 3 days ($t_{\text{pre-eq}}$).
201 When necessary, the pH value was re-adjusted by adding very small volumes of a 0.1M HCl or
202 0.1M NaOH solution in the tubes. After pre-equilibration, a given volume of a U(VI) stock
203 solution (with $[U] = 4.61 \times 10^{-3}$ M, solution acidified at pH 1 by HCl) was introduced in the
204 individual tubes to achieve defined $[U]_{I, aq}$ values. The tubes were then gently rotated end-over-
205 end and shaken during 4 days. After this contact time (t_R), the final pH of the suspensions was

206 measured. Solid-solution separation was achieved by a 3 hours centrifugation at 9000 rpm of
207 the individual tubes containing the suspensions (illite cutoff: ca.16 nm). The supernatants were
208 then removed from the individual tubes. For each supernatant, a given volume was taken for
209 electrophoretic mobility (EM) measurement and another one was acidified (using a 2% HNO₃
210 solution) for analysis of final aqueous concentration of U(VI) (noted here as [U]_{F,aq}). Each
211 experiment was carried out in duplicate. Blank experiments without solid were also performed
212 in a similar way than described above.

213 2.2.2 Uranyl and phosphate ions (co)sorption and desorption

214 Sorption experiments were conducted to investigate the effect of the presence of phosphate
215 ligands on the uptake of uranyl ions in NaIdP–electrolyte solution (0.005 M NaCl) systems, at
216 a given clay-to-solution ratio ($R_{S/L} = 3 \text{ g.L}^{-1}$). First, sorption edges (pH 3-8) of U(VI) and P(V)
217 were obtained at two different concentrations of total U ($[U]_{I,aq} = 1$ and $12 \text{ }\mu\text{M}$, respectively)
218 and a moderate concentration of total P ($[P]_{I,aq} = 100 \text{ }\mu\text{M}$). Second, sorption isotherms of uranyl
219 ions ($[U]_{I,aq}$ varying in the range 1-12 μM) were obtained at pH 4 and at two P concentrations
220 ($[P]_{I,aq}$: 20 and 100 μM , respectively). Experiments were conducted as described cf. §2.2.1
221 except that known volumes of stock solutions of phosphate ions and uranyl ions, respectively,
222 were added simultaneously to the individual tubes in order to achieve desired $[P]_{I,aq}$ and $[U]_{I,aq}$
223 values. Two of the co-sorption experiments (pH_F equal to 5.2 and 4.1, respectively) were used
224 for studying the kinetics of desorption of U(VI) and provide information on the reversibility of
225 the (co)sorption processes. After the step of equilibration of the two above-mentioned sorption
226 experiments, the pH of the suspensions were brought to a value of 3.2 in the individual tubes.
227 The tubes were then gently rotated end-over-end and shaken during ca. 15 days. Aliquots of the
228 suspensions were regularly taken for solid-solution separation by centrifugation.

229 2.3 Sample analyses

230 At the end of each experiment, the supernatant of the centrifuged sample was taken for EM
231 measurements (Zetasizer Nano equipment Malvern, three measurements per sample) and an
232 aliquot was also diluted with 2% HNO₃ prior to its analysis by ICP-MS to determine final
233 aqueous concentration of U ([1]). Each supernatant was also analyzed by ion chromatography
234 to determine final concentration of phosphate ions (Eco IC, Metrohm, analytical uncertainties:
235 1–10%). Percentage (%) and amount (μmol. g⁻¹) of sorbates sorbed were calculated as follows:

$$236 \quad \% \text{ sorbed} = \frac{C_i - C_{eq}}{C_i} \times 100 \%$$

$$237 \quad \text{Amount sorbed} = (C_i - C_{eq}) \times \frac{V}{M}$$

238 C_{init.} and C_{eq} are the initial and final aqueous concentration of sorbate (μmol.L⁻¹), respectively,
239 V the volume of solution (in L) and M the mass of solid sample (in g). Uncertainties on the
240 percentage of sorption and surface coverage were estimated to be lower than 10% for U and P.

241 2.4 In-situ ATR FTIR spectroscopy experiments

242 The methods used and results obtained from ATR FTIR experiments carried out to monitor in
243 situ the sorption of phosphate ions (20-250 μM) onto NaIdP, and to acquire reference data on
244 the IR vibrations of aqueous phosphate species, or changes in (Na)IdP (surface) structures
245 during sorption, are detailed elsewhere ([1]). In the present study, experiments were performed
246 to monitor by ATR FTIR spectroscopy the in situ evolution of (Na)IdP - solution interface
247 during (co)sorption of trace level of U(VI) ([U]_{I,aq} : 2-10 μM), in the presence of phosphate ions
248 ([P]_{I,aq} : 100 μM). Complementary “blank” experiments were performed to get reference data
249 on IR vibrations of aqueous uranyl phosphate species and/or on possible U(VI)-phosphate
250 precipitates formed directly from experimental solutions. Each IR spectrum (an average of 2000
251 scans/spectrum, resolution of 4 cm⁻¹) was collected during 20 minutes.

252 2.4.1 Monitoring of the clay–solution interface along sorption

253 The method used to cover the ATR crystal with a two-layers NaIdP–solution system is
254 described in details in a previous study ([1]). Briefly, the method consisted in equilibrating a
255 clay-solution system in a polyethylene tube by gentle shaking during 3 days (at pH 4 and $R_{S/L}$
256 = 3 g.L⁻¹). Then, the suspension was introduced in the ATR cell and the clay particles were let
257 to sediment onto the ZnSe crystal during 3 days. A reference baseline was taken before starting
258 the sorption experiment. The whole procedure was shown to yield nearly equilibrated clay –
259 solution systems, leading to insignificant contributions of IR vibrations originating from illite
260 dissolution and / or (surface) re-organization to the FTIR spectra recorded during sorption ([1]).
261 Two ATR FTIR experiments were performed to gain insights into the effects of key parameters.
262 The first experiment was carried out to monitor changes in coordination environments of sorbed
263 P along an increasing of $[U]_{I,aq}$ (2-10 μ M) as follows. First, 100 μ M of aqueous P was added to
264 an equilibrated NaIdP–electrolyte solution bilayer system in the ATR cell (two successive
265 additions of a small volume of a stock phosphate solution to reach a $[P]_{I,aq}$ value of 50 μ M and,
266 after twenty minutes, of 100 μ M). The FTIR interface spectra were recorded during 2 hours.
267 Second, the concentration of U in the ATR cell was progressively increased by stepwise
268 additions of small volumes of a U stock solution (increase of $[U]_{I,aq}$ by 2 μ M per hour). After
269 each addition, FTIR interface spectra were recorded. The second experiment aimed at
270 monitoring the NaIdP-solution interface as a function of reaction time ($t_R = 3$ days) along the
271 process of (co)sorption of phosphate ions and uranyl ions (simultaneous additions in the ATR
272 cell of small volumes of the P stock solution and U stock solution to reach values of $[U]_{I,aq}$ of 8
273 μ M and $[P]_{I,aq}$ of 100 μ M, and recording of FTIR interface spectra during 3 days).

274 2.4.2 Blank ATR FTIR experiments

275 ATR FTIR spectroscopy analyses of solutions were made (in the absence of clay) in order: (i)
276 to obtain IR spectra of reference for aqueous complexes formed between uranyl ions and
277 phosphate ligands and/or to identify possible U(VI)-phosphate precipitates likely to form under
278 certain conditions, and (ii) to determine detection limits for the U(VI) phosphato species /
279 precipitates. Uranyl phosphate solution species were studied at pH 4, for a given aqueous
280 phosphate concentration ($[P]_{l, aq} = 100 \mu\text{M}$) and an increasing of $[U]_{l, aq}$ (from 2 to 8 μM) that
281 were similar to those investigated in the first ATR FTIR sorption experiment (cf. §2.4.1).
282 Desired volumes of stock solutions of P and U(VI) were added simultaneously to a 0.005 M
283 NaCl electrolyte solution in the ATR cell and the IR spectra were recorded ($t_R < 4$ hours).

284 2.4.3 Analysis of the FTIR spectra

285 Analysis of the FTIR spectra recorded was focused on the mid-infrared region $900\text{--}1200 \text{ cm}^{-1}$
286 which is characterized by the presence of the ν_3 P-O(M) antisymmetric stretching and / or ν_1 P-
287 O(M) symmetric stretching (M: hydrogen or metal atom) vibration bands [75,76]. The
288 OriginPro version 9.1 software was applied for baseline correction and decomposition of IR
289 spectra to identify IR peaks (Gaussian lines and least-square fitting). Adjustable parameters
290 (such as position, intensity, and width of bands) were kept free during spectra decomposition.
291 Only in few spectra showing very low absorbance, the band position was adjusted. In previously
292 published studies of phosphate sorption onto Fe- and Al- (hydro)oxides, band's number and
293 position in the region $900\text{--}1200 \text{ cm}^{-1}$ were widely used in consideration of phosphate molecular
294 symmetry [75–79]. In addition, $\delta(\text{P-OH})$ bending band may be present as a broad band at 1220--
295 1240 cm^{-1} in IR spectra of aqueous species as H_2PO_4^- and H_3PO_4^0 [78,80] and / or outer sphere
296 phosphate surface species formed at mineral minerals. Previously published studies of uranyl
297 coordination environments by using vibrational spectroscopy were mainly focused on the

298 infrared-active U-O antisymmetric stretching band (ν_3) observable at 900–980 cm^{-1} and on the
299 Raman-active U-O symmetric stretching band (ν_1) at 800–880 cm^{-1} [81,82]. For complexes of
300 uranyl ions formed in solution or at mineral surface, the ν_3 of the uranyl unit was found to be in
301 the range 890–954 cm^{-1} and the ν_1 in the range 834–870 cm^{-1} [55,82,83]. The ν_3 band of uranyl
302 unit was expected to be not easily observable in IR spectra of NaIdP–solution systems, due to
303 a high IR absorption of clays at $\sim 950 \text{ cm}^{-1}$ (e.g., [84]) and to our system cutoff at $\sim 900 \text{ cm}^{-1}$.

304 2.4.4 Short overview of published IR data on uranyl and phosphate species

305 *Phosphate ions.* A short summary of the molecular symmetry analysis of PO_4 unit in phosphate
306 ions is given here, based on previously published papers [75–77,85]. Aqueous phosphate
307 speciation in 0.005 M NaCl electrolyte solution is dominated at $\text{pH} > 12$ by PO_4^{3-} ions, which
308 have a T_d molecular symmetry. These unprotonated phosphate ions have two IR-active IR bands
309 corresponding to antisymmetric bending at 567 cm^{-1} (T_2 , ν_4) and antisymmetric stretching at
310 1006 cm^{-1} (T_2 , ν_3) [85]. The monoprotonated $\text{HPO}_4^{2-}(\text{aq})$ and triply protonated $\text{H}_3\text{PO}_4(\text{aq})$ ions are
311 main species at $\text{pH} 8\text{--}12$ and at $\text{pH} < 2$, respectively, and have a C_{3v} molecular symmetry. The
312 former has three IR-active bands: two ν_3 bands at 1077 (E) and 989 cm^{-1} (A_1) and one ν_1 band
313 at 850 cm^{-1} (A_1). The latter has two ν_3 at 1174 and 1006 cm^{-1} and one ν_1 at 890 cm^{-1} [75–77].
314 In the pH range 2–7, H_2PO_4^- ions are predominant phosphate species and display a C_{2v} molecular
315 symmetry. They have three ν_3 vibration bands at 1160 (A_1), 1074 (B_1), 940 (B_2) cm^{-1} and one
316 ν_1 band at 874 cm^{-1} (A_1) [77,85]. The number and bands' position of IR-active bands ν_3 and ν_1
317 of aqueous phosphate ions are references to be used in the analysis of molecular symmetry of
318 PO_4 unit in phosphate species sorbed at mineral–solution interfaces (for example, [78]) or
319 participating in aqueous complexes (for example, [75]).

320 *Uranyl ions.* Two vibration bands characteristics of the UO_2 unit, i.e., the antisymmetric band
321 ν_3 (IR active) and symmetric band ν_1 (Raman active), were widely used in molecular-scale

322 studies of the coordination environment of UO_2 in aqueous solution or in solid state [86]. Free
323 (hydrated) uranyl ion shows a ν_3 band at 962 cm^{-1} and a ν_1 band at 870 cm^{-1} [82]. Replacement
324 of equatorial water molecules of uranyl ions during their complexation by ligands leads to a
325 weakening of the $\text{U}=\text{O}_{\text{ax}}$ axial bonds, and consequently, bonds' lengths are increased and
326 positions of ν_3 and ν_1 bands are decreased (i.e., $\nu_3 < 962\text{ cm}^{-1}$ and $\nu_1 < 870\text{ cm}^{-1}$) [82]. The IR-
327 active band ($\nu_3, 962\text{ cm}^{-1}$) was studied here in blank ATR FTIR experiments.

328 *Uranyl-phosphate aqueous species and/or precipitates.* Nguyen Trun al [81] have investigated,
329 using Raman spectroscopy, aqueous uranyl complexes formed with different ligands such as F^- ,
330 Cl^- , Br^- , SO_4^{2-} , HSO_4^- , NO_3^- , ClO_4^- , CH_3CO_2^- and $\text{C}_2\text{O}_4^{2-}$. The authors studied shifts in ν_1 band
331 of UO_2 (Raman active, symmetry stretching of $\text{U}=\text{O}$) when varying solution parameters like
332 pH, ionic strength and ligand-to-uranyl ratios. Comarmond et al [54] have investigated aqueous
333 uranyl phosphate species at pH 4 (at $[\text{U}]_{\text{l, aq}} = [\text{P}]_{\text{l, aq}} = 20\text{ }\mu\text{M}$). These authors have indicated
334 that low solubility of U(VI)-phosphate aqueous complexes made it difficult to get vibrational
335 data. Nevertheless, they could observe that the IR spectra of a freshly prepared uranyl phosphate
336 solution was almost identical to that of a U(VI) phosphate precipitate (acquired after
337 ultracentrifugation of an aged U-P-solution system). They identified IR bands at 1125, 994 and
338 919 cm^{-1} and suggested to attribute the latter to the ν_3 band of UO_2 and the formers to ν_3 bands
339 of PO_4 units (having a C_{3v} molecular symmetry when coordinated to uranyl ions, likely in a
340 monodentate complexation mode). They have moreover identified by using TRIFS
341 spectroscopy the precipitates formed in their studied solutions as being $(\text{UO}_2)_3(\text{PO}_4)_2(\text{s})$. Similar
342 IR spectral features were observed for several U(VI) phosphates [87], for which the ν_3 bands
343 of UO_2 unit and PO_4 unit were found at $880\text{-}920\text{ cm}^{-1}$, at $995\text{-}1000$ and $1115\text{-}1123\text{ cm}^{-1}$,
344 respectively (e.g., at $915, 1000$ and 1120 cm^{-1} and $919, 995$ and 1123 cm^{-1} for meta-autunite,
345 $\text{Ca}(\text{UO}_2)_2(\text{PO}_4)_2 \cdot 6\text{-}8\text{H}_2\text{O}$, and sabugalite, $\text{HAl}(\text{UO}_2)_4(\text{PO}_4)_4 \cdot 6\text{-}8\text{H}_2\text{O}$, respectively).

346 **3 Results and discussion**

347 *3.1 Macroscopic sorption behavior of uranyl ions*

348 3.1.1 Uranyl sorption edges and isotherms

349 Fig. 1 shows the effects of pH on macroscopic (co)sorption of U(VI) at two total concentrations
350 ($[U]_{I, aq}$: 1 and 12 μM), in the presence or absence of phosphate ions ($[P]_{I, aq}=0$ or 100 μM), and
351 on particle EM in NaIdP - solution 0.005 M NaCl systems ($R_{S/L}$: 3 $\text{g}\cdot\text{L}^{-1}$, $t_R = 4$ days). There
352 were observed S-shaped uranyl sorption edges (Fig. 1a) whose values of pH_{50} (the pH at which
353 the percentage of U sorption is equal to 50%) are in the acidic pH domain. In the absence of P,
354 a ten-fold increase in $[U]_{I, aq}$ induces a small shift in the pH_{50} value (from ca. 3.9 to 4.1 for $[U]_{I, aq}$
355 increasing from 1 μM to 12 μM) and U(VI) uptake is almost complete in the pH range 6-8. This
356 suggests that multiple sorption species and/or clay surface sites are involved in the uptake of U
357 at $\text{pH} < 5$, in the range of U surface coverage studied ($< 3.8 \mu\text{mol}\cdot\text{g}^{-1}$, Fig. 1a). A limited change
358 in the respective contributions of high and low affinity surface sites at clay edge platelets are
359 likely. If considering a simple hypothesis, which is that each uranyl ion sorbed is bound to a
360 single sorption site at the clay surface, the calculated value of surface site occupancy by U is
361 found to be low (ca. 0.02 sites. nm^{-2}). This value is much lower than previously published values
362 reported in the literature, for example, for the density of total sites present at edges of illite
363 platelets (2.31 sites. nm^{-2} [88], 0.4 sites. nm^{-2} [50,89]), or low-affinity sites on clay basal planes
364 (13-16 sites. nm^{-2} [90]). Bradbury and Baeyens [50,89] considered in their modeling studies of
365 the sorption of uranyl ions and other trace metals onto Illite du Puy that a small amount (ca.
366 0.01 sites. nm^{-2} or $2 \mu\text{mol}\cdot\text{g}^{-1}$) of very high affinity sites were present at the clay edges, whose
367 total surface site capacity was much higher ($40 \mu\text{mol}\cdot\text{g}^{-1}$ for aluminol sites and $40 \mu\text{mol}\cdot\text{g}^{-1}$ for
368 silanol sites). Based on their work, it is expected that a small amount of high affinity surface
369 sites present on the edges of NaIdP particles may be involved in very strong interactions with
370 sorbates, and may control U(VI) sorption at the lowest U concentration studied here ($[U]_{I, aq}=1$

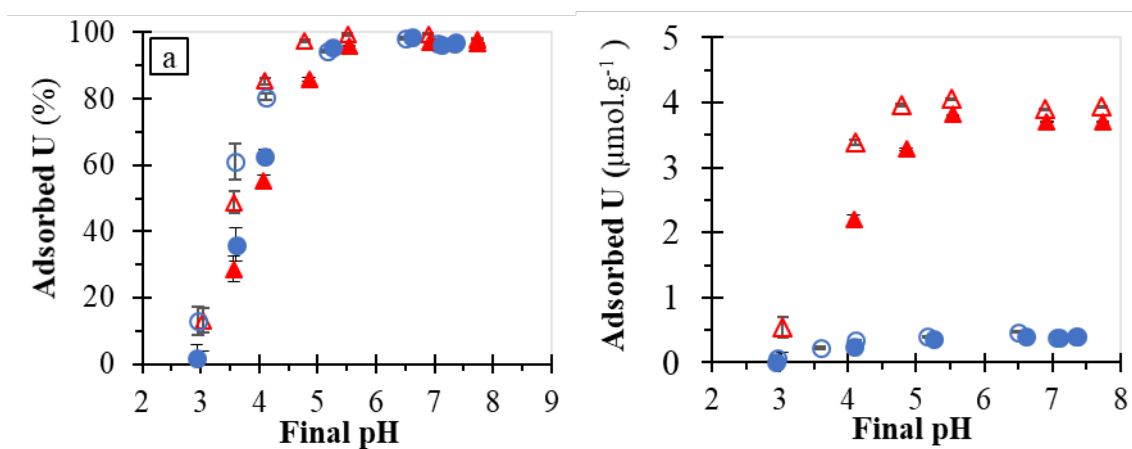
371 μM and $R_{S/L} = 3 \text{ g.L}^{-1}$, Fig. 1a). A limited fraction of low-affinity edge surface sites may
372 contribute to U sorption at a tenfold higher U concentration, which would be consistent with
373 the decrease in U sorption percentage observed upon increasing $[\text{U}]_{\text{I, aq}}$ in experiment, at a given
374 acid pH ($[\text{U}]_{\text{I, aq}} = 12 \mu\text{M}$, Fig. 1a). Complementary sorption isotherms acquired at pH 3, 3.5 and
375 4.1 over a wide range of U concentration ($[\text{U}]_{\text{I, aq}}$: 1-25 μM) are presented in the Supporting
376 Information (Figs. S1-S2). A slight increase in U sorption percentage was observed at the
377 highest U concentrations studied (at pH 4), as well as a non-linear increase in amount sorbed,
378 indicating the formation of additional uranyl sorption species at high U surface coverage,
379 possibly including U(VI) (surface) precipitates. The results obtained on the effect of a decrease
380 in $R_{S/L}$ (from 3 to 1 g.L^{-1}) on the sorption edges of U(VI) confirm that a small number of very
381 high-affinity sites is available for U sorption on the edges of NaIdP, consistently with published
382 studies [50,89] (Figs. S3-S4 in Supporting Information). At low U concentration ($[\text{U}]_{\text{I, aq}} = 1 \mu\text{M}$),
383 a decrease in $R_{S/L}$ had no or little effect on U sorption edges and U coverage values of the clay
384 surface. High-affinity surface sites may therefore be primarily responsible for the sorption of
385 trace amounts of U onto the clay edge platelets under these conditions. In contrast, a decrease
386 in $R_{S/L}$ for a tenfold concentration of U in the experiments ($[\text{U}]_{\text{I, aq}} = 12 \mu\text{M}$) induced a significant
387 shift in the position of the U sorption edge (from 4.1 to 4.8) and a non-linear increase in U
388 surface coverages (at $\text{pH} > 5$). Uranyl ion sorption, at high U concentration and low $R_{S/L}$, can
389 therefore lead to saturation of high affinity sites and may involve multiple types of surface sites
390 and/or uranyl sorption species.

391 ***3.1.1 Effect of uranyl sorption on electrophoretic mobility***

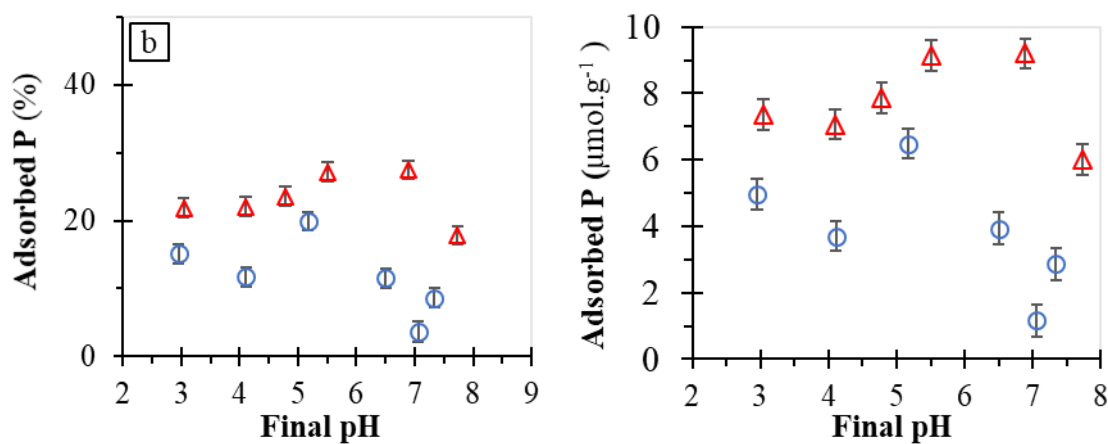
392 EM measurements of NaIdP suspensions (pH: 3-8, $R_{S/L}$: 3 g.L^{-1} in 0.005 M NaCl electrolyte
393 solution) have been detailed previously ([1]). The isoelectric point (IEP) of NaIdP, *i.e.*, the pH
394 at which EM and surface potential are equal to zero, was found to be low ($\text{pH}_{\text{IEP}} \sim 3$). EM was
395 shown to diminish with pH due to deprotonation of amphoteric I (silanol, aluminol or ferrinol)

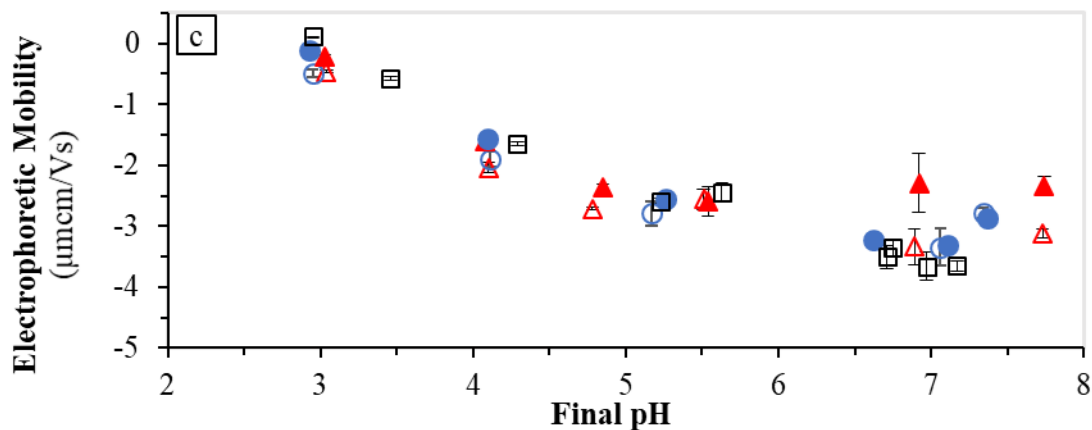
396 surface sites. Results obtained here on the effect of U(VI) sorption on EM values are given in
397 Fig. 1c, where they are compared to EM values acquired previously in the absence of phosphate
398 and / or uranyl ions. There was observed that sorption of 1-12 μM of U(VI) at acidic pH has no
399 significant effect on EM, within our experimental uncertainties. A small effect is visible at near-
400 neutral pH (~ 7) where the quantitative sorption of U induces an EM increase (for $[\text{U}]_{\text{I,aq}} = 12$
401 μM), which suggests the formation of U sorption species that impart positive charges to the
402 clay surface.

403



404





405
 406 **Fig. 1** Macroscopic sorption of uranyl ions (a) and phosphate ions (b), and electrophoretic
 407 mobility (c), vs final pH, for experiments performed in NaIdP-solution systems at different total
 408 U(VI) concentrations, in the absence or presence of phosphate ions. Conditions: NaIdP-to-
 409 solution ratio, $R_{S/L}$, of $3\text{g}\cdot\text{L}^{-1}$; 0.005M NaCl electrolyte solution; reaction time, t_R , of 4 days;
 410 pre-equilibration time of NaIdP-electrolyte systems prior to sorbate addition, $t_{\text{pre-eq}}$, of 3days.
 411 (○: $[\text{U}]_{\text{I,aq}} = 1\mu\text{M}$ and $[\text{P}]_{\text{I,aq}} = 100\mu\text{M}$; △: $[\text{U}]_{\text{I,aq}} = 12\mu\text{M}$ and $[\text{P}]_{\text{I,aq}} = 100\mu\text{M}$; ▲, ● without
 412 P; □: Blank). EM data of blank experiments without U and P (×) taken from [1].

413 3.1.2 Effect of phosphate ligand on the macroscopic sorption of U

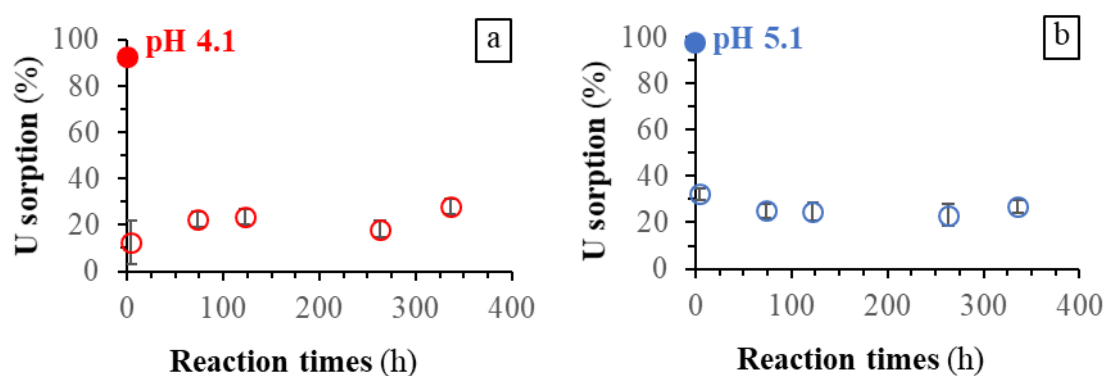
414 Fig. 1a shows that the presence of phosphate ions ($[\text{P}]_{\text{I,aq}} = 100\mu\text{M}$) resulted in a significant
 415 shift of U(VI) sorption edges towards lower pH values (for $[\text{U}]_{\text{I,aq}} = 1$ and $12\mu\text{M}$). At acidic pH,
 416 significant increases in the surface coverage of clay by U were observed ($3\text{-}4\mu\text{mol U}\cdot\text{g}^{-1}$ at pH
 417 4-5 and $[\text{U}]_{\text{I,aq}} = 12\mu\text{M}$). Hence, at acidic pH, the presence of P promoted the sorption of U(VI)
 418 onto NaIdP. An increase in the percentage of P sorbed and clay surface coverage by P (of ca. 2
 419 and $6\mu\text{mol P}\cdot\text{g}^{-1}$ at acid and near-neutral pH, respectively) were also observed with increasing
 420 U concentration in the experiment (Fig. 1b and Figs. S5-6 in Supporting Information). Thus,
 421 the increase in U sorption observed when phosphate ligands were added to NaIdP-solution
 422 systems was probably due to the formation of (multiple) uranyl phosphate ternary surface
 423 complexes and/or U(VI) phosphate surface precipitates. Fig. 1c shows that the presence of

424 phosphate ligands slightly decreases the EM values of clay particles in the pH range studied,
425 *i.e.*, it confers negative charges on the clay surface, suggesting the involvement of phosphate
426 anions in the surface species formed. Furthermore, based on published values for the high
427 affinity surface sites of the conditioned Illite du Puy (about $2 \mu\text{mol.g}^{-1}$ or $0.01 \text{ sites.nm}^{-2}$,
428 [50,89]), we can hypothesize that uranyl phosphate surface complexes formed on NaIdP may
429 involve high-affinity and low-affinity hydroxyl (amphoteric) sites present on the clay edge
430 platelets, for high $[\text{U}]_{\text{I,aq}}$ and $[\text{P}]_{\text{I,aq}}$ values used in the experiments. Complementary U sorption
431 isotherms acquired for a wide range of U concentrations (Figs. S1 and S2, Supporting
432 Information) show that, at acidic pH, the promotion of U(VI) sorption upon addition of
433 phosphate ligands is higher at high U concentrations ($[\text{U}]_{\text{I,aq}} \geq 12 \mu\text{M}$) than at the low
434 concentration, suggesting that multiple uranyl phosphate species are successively formed in
435 NaIdP-phosphate-solution systems when $[\text{U}]_{\text{I,aq}}$ increases. Since limited formation of uranyl
436 phosphate colloidal phases was observed in the absence of NaIdP (5-10% of total U, for
437 $[\text{U}]_{\text{I,aq}}=1-10 \mu\text{M}$ and $[\text{P}]_{\text{I,aq}}=100 \mu\text{M}$, Fig. S7 in Supporting Information), the contribution of a
438 U(VI) phosphate precipitation mechanism from supersaturated solutions cannot be excluded to
439 explain the increased retention of U observed in NaIdP - phosphate - solution systems at the
440 highest value of $[\text{U}]_{\text{I,aq}}$ studied ($25 \mu\text{M}$).

441 3.1.3 Reversibility of the sorption of U in the presence of phosphate ligands

442 The results of the desorption experiments of uranyl ions ($[\text{U}]_{\text{I,aq}} = 12 \mu\text{M}$) previously sorbed
443 after a reaction time of 4 days and at pH values of ~4 and ~5, respectively, and in the presence
444 of phosphate ligands ($[\text{P}]_{\text{I,aq}} = 100 \mu\text{M}$), are presented in Fig. 2. A sharp decrease in the
445 percentage of U sorption was observed when the experimental pH was reduced from its initial
446 value to 3.2. Desorption of U(VI) was found to be rapid and almost complete within a few hours.
447 In fact, the percentage of total U retained at pH 3 on the clay surface after a few hours desorption
448 was found to be around 20% (which is slightly higher than the percentage of U sorption at pH

449 3 under similar conditions of U and P concentrations, see Fig. 1a). This finding provides
 450 evidence that the U-P co-sorption prevalent under the conditions studied proceeds mainly by
 451 reversible surface reactions, such as surface complexation reactions. This supports the
 452 hypothesis of the formation of ternary surface complexes of uranyl phosphate on NaIdP at acid
 453 pH and at low U concentrations ($\leq 12 \mu\text{M}$), possibly onto hydroxyl sites present on the clay
 454 edges, and rules out the formation of a significant amount of uranyl phosphate (surface)
 455 precipitates, under the conditions studied.



456
 457 **Fig. 2** Results on the desorption kinetics of U(VI) previously sorbed on NaIdP, in the presence
 458 of phosphate ions, at a pH of (a) 5.1 and (b) 4.1 (full circles), after decreasing the experimental
 459 pH to a value of 3.2 (empty circles). Conditions: $[\text{P}]_{\text{I, aq}} = 100 \mu\text{M}$, $[\text{U}]_{\text{I, aq}} = 12 \mu\text{M}$, $R_{\text{S/L}} = 3 \text{g.L}^{-1}$,
 460 0.005M NaCl electrolyte solution.

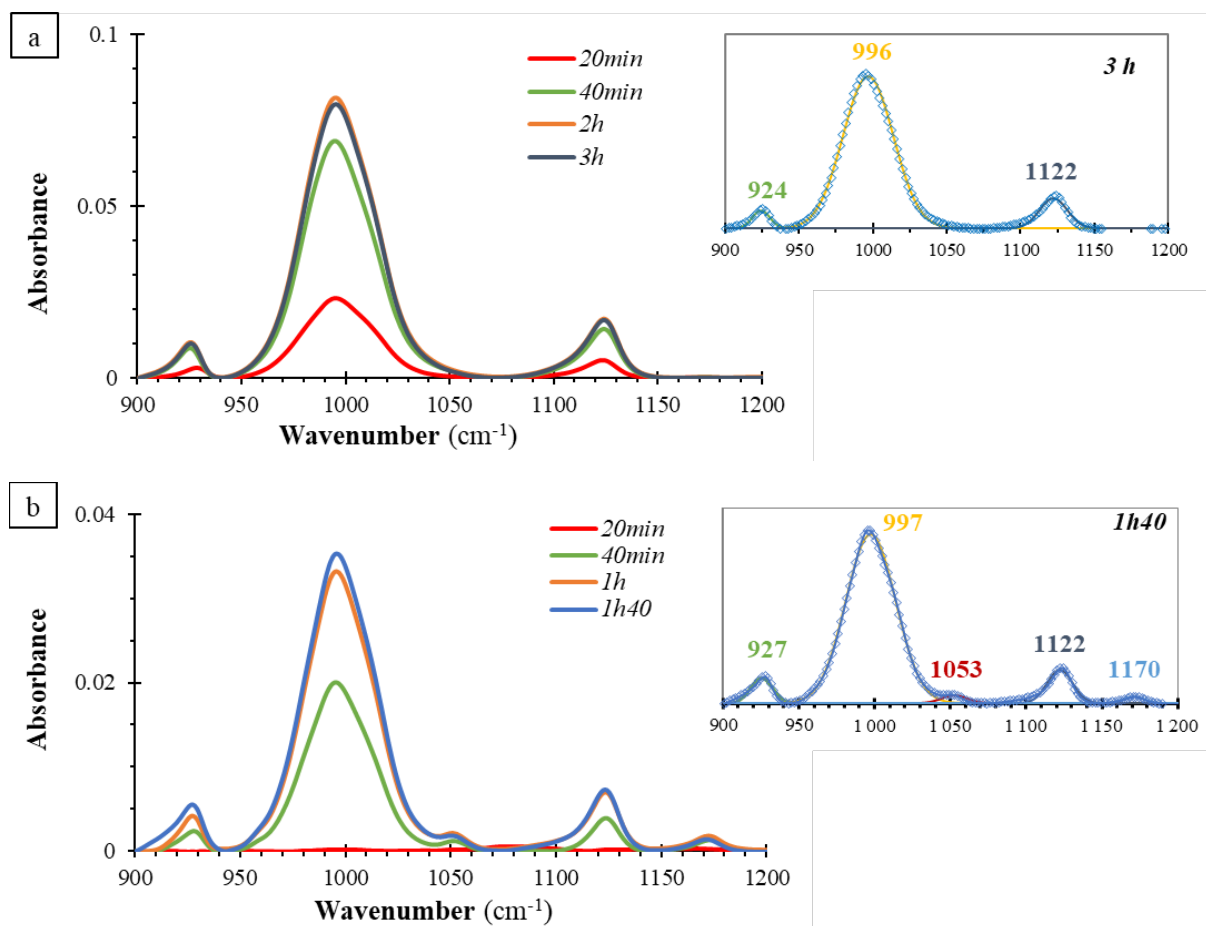
461 3.2 *In situ* ATR FTIR study of uranyl-phosphate surface species

462 3.2.1 Reference IR spectra of uranyl phosphate solution species

463 The aqueous speciation of U(VI) in the presence of phosphate ligands ($[\text{U}]_{\text{I, aq}} = 2 \mu\text{M}$ and 10
 464 μM ; $[\text{P}]_{\text{I, aq}} = 100 \mu\text{M}$) calculated by using the Visual MINTEQ code, and the database used, are
 465 reported in Supporting Information (Figs. S8-S9 and Table S1, respectively). In the pH range
 466 4-8, the major aqueous species are: UO_2^{2+} ($\text{pH} < 4$), $\text{UO}_2\text{HPO}_4(\text{aq})$ ($4 < \text{pH} < 6$), UO_2PO_4^- ($6 < \text{pH} < 7$)
 467 and $(\text{UO}_2)_2\text{CO}_3(\text{OH})_3^-$ ($7 < \text{pH} < 8$). Fig. 3a reports ATR FTIR spectra (in the wavenumber region
 468 $900\text{-}1200\text{cm}^{-1}$) collected during 3 hours for solutions at pH 4 containing uranyl and phosphate

469 ions ($[U]_{l,aq} = 8 \mu\text{M}$, $[P]_{l,aq} = 100 \mu\text{M}$). The spectra show the appearance of IR absorption bands
470 whose intensities were increasing during the first two hours. Three bands were observable, with
471 the most intense one being positioned at 996 cm^{-1} and the others at 1122 and 924 cm^{-1} . It should
472 be noted that the absorbance of these bands is at least two orders of magnitude higher than that
473 of vibrational bands recorded for the aqueous phosphate species H_2PO_4^- , under similar
474 conditions and in the absence of U ([1]), certainly due to formation of uranyl phosphate aqueous
475 complex and / or precipitate. FTIR spectra of uranyl phosphate complexes and/or precipitate(s)
476 forming in solution at pH 4 and at the higher U concentration studied ($[U]_{l,aq} = 8 \mu\text{M}$) are shown
477 in Fig.3b. An increase in the intensity of the IR absorption bands was observed during the first
478 2 hours, due to increasing formation of the uranyl phosphate complexes / precipitates. In
479 addition to the three above-mentioned IR bands (at 996 , 1122 and 924 cm^{-1}), two other weak
480 vibrational bands were observable. Weak intensities of the latter made it difficult to determine
481 precisely the position of their maxima (at ca. 1055 and 1170 cm^{-1} , respectively). These bands
482 could possibly be ascribed to an aqueous U-P species whose $\nu_3(\text{P-O})$ bands are slightly shifted
483 compared to those reported (at 1075 and 1160 cm^{-1}) for the diprotonated phosphate ion (H_2PO_4^- ,
484 C_{2v}), which is the dominant aqueous phosphate species at pH 4. Maxima positions and relative
485 intensities of the main bands (at 996 cm^{-1} , 1122 and 924 cm^{-1}) are consistent with previously
486 published IR data by Čejka et al. [87] and Comarmond et al. [54] for uranyl phosphate aqueous
487 complexes and/or of U(VI) phosphate minerals, which display almost similar IR features (cf.
488 §2.4.4). Formation of a U(VI)-phosphate phase is in agreement with calculations indicating that
489 solution used in experiment (at $[U]_{l,aq} = 8 \mu\text{M}$ and $[P]_{l,aq} = 100 \mu\text{M}$) was highly over-saturated
490 with regard to a U(VI) phosphate mineral, namely $(\text{UO}_2)_3(\text{PO}_4)_2(s)$, and slightly oversaturated
491 with respect to Na-autunite (Supporting Information, Table S2). Moreover, batch experiments
492 conducted without clay indicated the formation of uranyl phosphate colloids (Supporting
493 Information, Fig. S7) at pH 4, which would represent ca. 5% of total U. Concerning IR spectra

494 of U(VI) in electrolyte solutions containing no phosphate ligands, no absorption bands were
495 observable for $[U]_{I,aq} \leq 10 \mu\text{M}$ (data not shown). These FTIR results on uranyl phosphate
496 solution speciation is further discussed in §4.1.



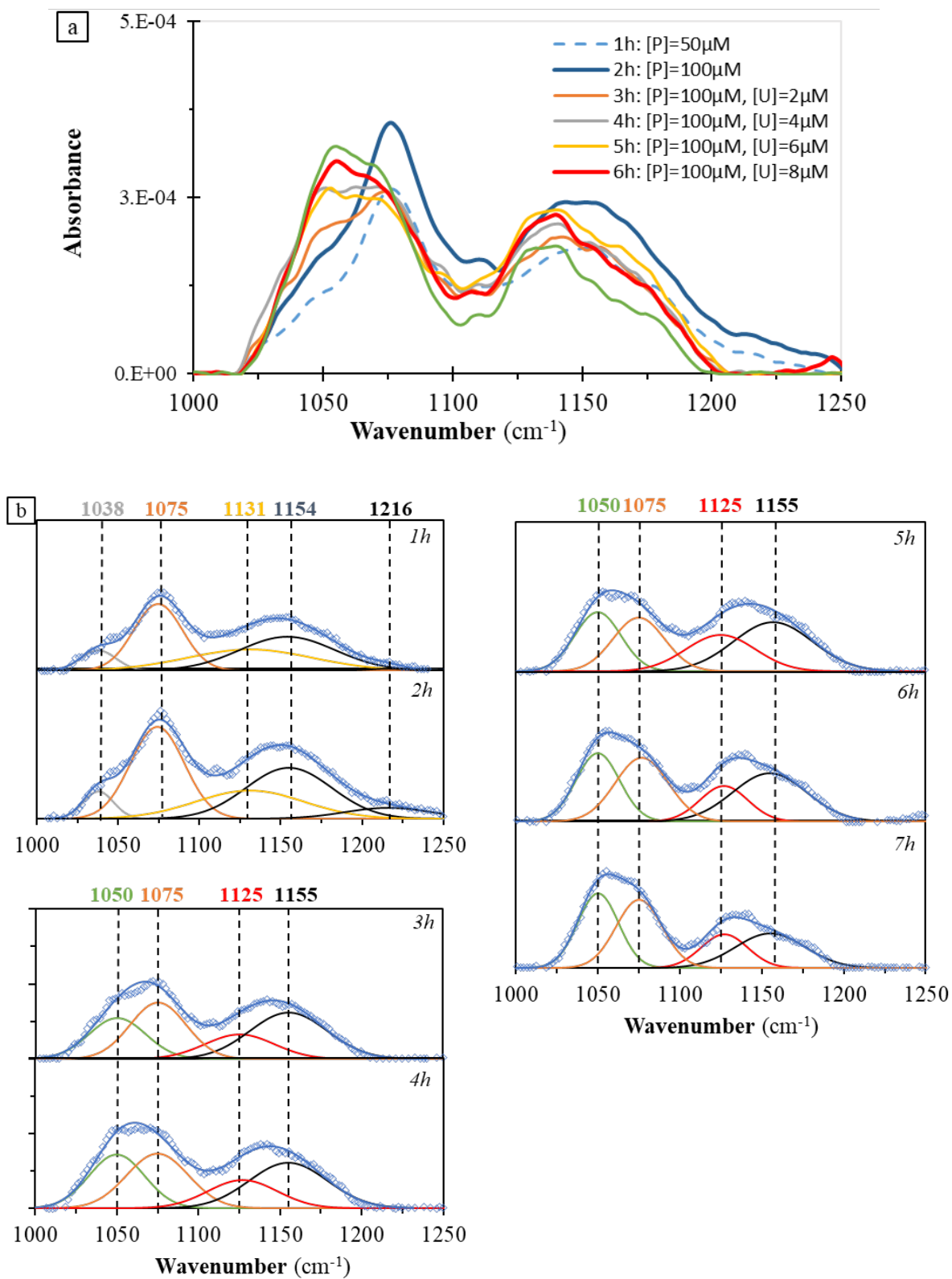
497
498 **Fig. 3** FTIR spectra of uranyl phosphate solution species recorded at different reaction time (t_r)
499 after simultaneous addition of phosphate ions ($[P]_{I,aq} = 100 \mu\text{M}$) and uranyl ions at (a) $[U]_{I,aq} =$
500 $2 \mu\text{M}$ and (b) $[U]_{I,aq} = 8 \mu\text{M}$, to a 0.005 M NaCl electrolyte solution at pH 4, in the ATR cell
501 (inserts : FTIR spectra decomposition).

502 3.2.2 In situ ATR FTIR experiments of (co)sorption of uranyl and phosphate ions

503 *Effects of uranyl concentration.* NaIdP-phosphate-solution interface was monitored along an
504 increase in the total concentration of U(VI) (from 0 to 8 μM). After two successive additions
505 of 50 μM of phosphate ions in the equilibrated bilayer NaIdP - solution system in the ATR cell,

506 spectral data were recorded during a reaction time of 2 hours (spectra 1 and 2, Fig. 4a). A well-
507 defined band with a peak maximum at 1075 cm^{-1} and a broad band at $1100 - 1250\text{ cm}^{-1}$, whose
508 intensity increased with time, were observed. Based on spectra decomposition shown in Fig.
509 4b, five IR absorption bands' maxima were identified (at 1037 , 1075 , 1132 , 1157 and 1215 cm^{-1}).
510 ¹). These data are consistent with those obtained in our previous ATR FTIR experiments of
511 phosphate ion sorption on NaIdP at acid pH ([1]). Briefly, these bands were attributed to
512 formation of an outer sphere surface complex (OSSC) of phosphate formed at low reaction time
513 and/or low phosphate concentration (referred "P-species A", with IR bands at 1075 , 1157 and
514 1215 cm^{-1}), with band positions similar to those of aqueous H_2PO_4^- species. This OSSC was
515 found to convert slowly (during ca. 1 day) into inner-sphere surface complexes of phosphate
516 forming at high affinity sites present of clay edge platelets (referred "P-species B", with ν_3 P-
517 O bands at 1003 , 1035 cm^{-1} , and another one with a ν_3 P-O band at 1132 cm^{-1}). P-species B
518 were shown to dominate the phosphate surface speciation at high values of $[\text{P}]_{\text{I, aq}} (> 250\mu\text{M})$
519 and/or t_{R} (3 days, at $[\text{P}]_{\text{I, aq}} = 100\mu\text{M}$), in the absence of U ([1]). The IR interface spectra
520 recorded herein during a stepwise increase of U(VI) concentration (by $2\text{ }\mu\text{M}$ per hour) in a
521 NaIdP – phosphate - solution system are given in Fig. 4a (spectra 3 to 7, $t_{\text{R}} = 7\text{ h}$). After first U
522 addition (at $t_{\text{R}} = 2\text{ h}$), there was observed the progressive disappearance within one hour of the
523 P-species B bands (at 1037 and 1132 cm^{-1}) and the appearance on the left-hand side of the band
524 at 1075 cm^{-1} of a shoulder, which becomes a band with a maximum at ca. 1050 cm^{-1} . Such a
525 disappearance of OSSC of phosphate, -and shift from 1037 to ca. 1050 cm^{-1} -, provides strong
526 evidence of a change in the coordination environment of sorbed PO_4 units upon addition of U.
527 The intensity of the band at 1050 cm^{-1} increased with increasing U(VI) concentration, although
528 absorbance remained fairly low and spectra rather noisy. Nevertheless, the existence and the
529 growth of this IR band provided evidenced for formation of uranyl-phosphate surface species
530 at the illite surface within a few hours. This band was not observed on IR interface spectra

531 recorded in NaIdP – phosphate - solution systems without U, neither at short reaction times
532 (spectra 1-2 in Fig. 4a) nor at longer reaction times up to 3 days ([1]). This band cannot be
533 attributed to a change in the configuration of surface hydroxyl groups with time ([1]) or with
534 sorption of U(VI), as it was not detected on the IR interface spectra recorded during U(VI)
535 sorption experiments on NaIdP performed at $[P]_{I, aq} = 0$ (data not shown). Spectra decomposition
536 results (Fig. 4b) show the presence on the FTIR interface spectra of a small band centered at
537 $\sim 1126 \text{ cm}^{-1}$, too, which could be also assigned to the ν_3 P-O vibration mode and whose weak
538 absorbance was independent of uranyl concentration. Possibly, this band corresponds to a
539 uranyl phosphate surface species (“U-P species A”) formed in limited amount and at low U
540 concentration. The bands at 1075 and 1157 cm^{-1} of P-species A, the OSSC of phosphate,
541 showed a small decrease in intensity with increasing $[U]_{I, aq}$, concomitantly to the increase of
542 the band at 1050 cm^{-1} . These results provide evidence of increasing formation with $[U]_{I, aq}$ of a
543 uranyl phosphate surface species that has a main IR band at 1050 cm^{-1} (referred to as “U-P
544 species B”). In summary, the IR data recorded at the NaIdP–U-P-solution interface, as a
545 function of uranyl ion concentration and for a short reaction time ($t_R < 7\text{h}$), show : (1) the fast
546 formation of an OSSC of phosphate (P-species A having IR bands at 1075 and 1160 cm^{-1})
547 before U addition and an ISSC of phosphate (P-species B having IR bands at 1075 and 1160
548 cm^{-1}), (2) the fast formation of a uranyl phosphate surface species formed in limited amounts
549 (U-P species A with a band at 1125 cm^{-1}) and another uranyl phosphate surface species (U-P
550 species B displaying a band at 1050 cm^{-1}), which occurs concomitantly to the disappearance of
551 P-species B (at $t_R < 3\text{h}$), and, (3) the growth of U-P species B with an increasing of U
552 concentration.



553

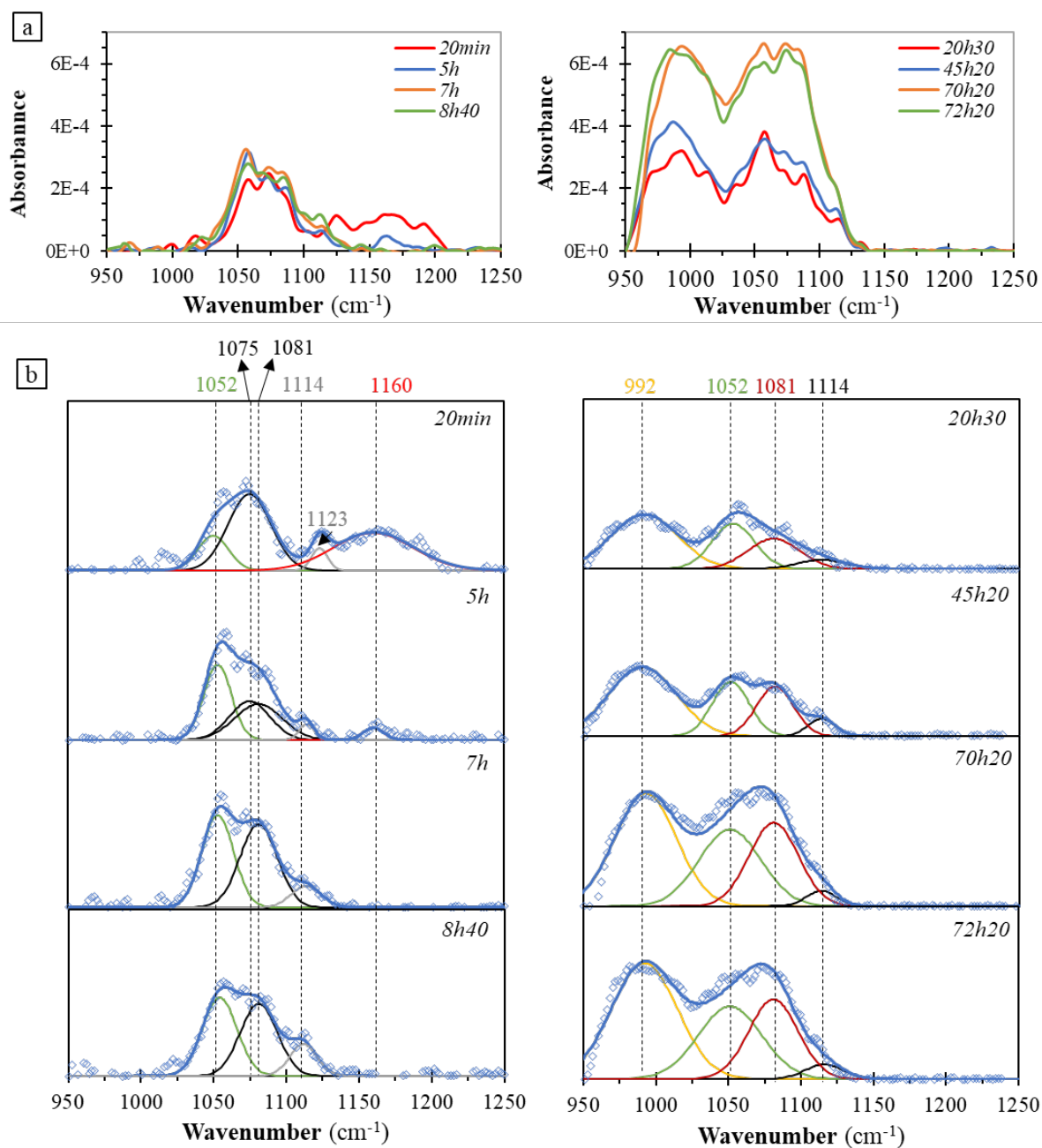
554 **Fig. 4** In situ ATR-FTIR interface spectra recorded with increasing U(VI) concentration, during

555 (co)sorption experiment of phosphate and uranyl ions added successively to a NaIdP-solution

556 bilayer system: (a) FTIR interface spectra and (b) spectra decomposition. Conditions: pH 4,
557 $[P]_{l,aq} = 50-100 \mu\text{M}$ (50 μM of P added at $t_R = 0$ and 1 h), $[U]_{l,aq} = 0, 2, 4, 6,$ and 8 μM (at $t_R =$
558 0-2, 3, 4, 5, and 6-7 h, respectively), $R_{S/L} = 3\text{g}\cdot\text{L}^{-1}$, 0.005M NaCl electrolyte. See main text and
559 §2.4.1 for experimental procedure.

560 *Effect of reaction time (t_R).* In situ ATR FTIR monitoring as a function of time ($t_R = 3$ days) of
561 the (co)sorption of uranyl and phosphate ions added simultaneously in a NaIdP–solution bilayer
562 system is illustrated in Fig. 5. A broad band with a low absorbance was observable in the range
563 of wavenumbers 1025 – 1125 cm^{-1} for spectra recorded within a reaction time of 20 hours. The
564 small band at 1123 cm^{-1} of “U-P species A” was observable only in the very short term. After
565 a t_R of 20 hours, there was observed a broad band exhibiting two maxima and extending
566 throughout the region of wavenumbers 950-1125 cm^{-1} , with its absorbance increasing with time
567 until stabilization at $t_R = 3$ days (Fig. 5a). For $t_R < 20$ h, spectra were decomposed in five bands
568 of weak absorbance and divided in two sets with maxima positions at 1075 and 1160 cm^{-1} , and
569 1053, 1081, 1114 cm^{-1} , respectively (Fig. 5b). All these bands can be assigned to ν_3 (P-O)
570 vibration bands, based on the comparison with IR spectra of aqueous phosphate species [77,78].
571 As described previously, the former set of bands is assigned to an OSSC of phosphate (P-species
572 A, [1]) and / or to H_2PO_4^- species in solution, because the bands’ position of these two types of
573 phosphate species are expected to be similar. These bands displayed a decrease in intensity with
574 t_R and were not observable anymore at $t_R > 7$ hours, while the other bands (at 1053 and
575 1081 cm^{-1} and the small one at 1114 cm^{-1}) showed an intensity increase with t_R . The IR band at
576 $\sim 1055 \text{cm}^{-1}$ remained constant after 7 h and it was assigned to the U-P species B. As shown in
577 the previous experiment, its appearance coincided with the introduction of uranyl ions in the
578 NaIdP – phosphate - solution system and its intensity was growing with U concentration (but
579 stabilized after one day). The well-defined band at 992 cm^{-1} in Fig. 5 was observable at $t_R > 20$
580 hours and its intensity increased concomitantly with that of the band at 1081 cm^{-1} along the

581 sorption process, i.e., up to $t_R \sim 3$ days. These two bands, and the small band at 1114 cm^{-1} , are
582 tentatively gathered and attributed to P-O vibrations of a single uranyl phosphate surface
583 species formed at a long reaction time (referred to as “U-P species C”), due to their similar
584 evolution during sorption. In summary, the IR data recorded during (co)sorption of uranyl and
585 phosphate ions at the NaIdP–solution interface as a function of time (3 days) show : (1) the
586 presence at a short reaction time of an OSSC phosphate species that disappears rapidly ($t_R < 5\text{h}$)
587 (P-species A with IR bands at 1075 and 1160 cm^{-1}), (2) the formation at a short reaction time
588 of a uranyl phosphate surface species formed in limited amounts (U-P species A with a band at
589 1125 cm^{-1}), (3) the formation of a uranyl phosphate surface species (U-P species B with a main
590 band at 1052 cm^{-1}) whose growth stabilizes after $t_R = 1$ day, (3) the late appearance (at $t_R = 1$
591 day) and growth with time of an uranyl phosphate surface species that becomes dominant at
592 long t_R (U-P species C with IR bands at 992 , 1081 and 1114 cm^{-1}).



593

594 **Fig. 5** In situ ATR FTIR interface spectra recorded as a function of reaction time, during an
 595 experiment of the (co)sorption of phosphate ions and uranyl ions added simultaneously to a
 596 NaIdP–solution bilayer system: (a) FTIR interface spectra (8 points- Savitzky-Golay algorithm
 597 smoothed) and (b) spectra decomposition. Conditions: pH 4, $[U]_{l,aq} = 8 \mu\text{M}$, $[P]_{l,aq} = 100 \mu\text{M}$,
 598 $R_{S/L} = 3 \text{ g}\cdot\text{L}^{-1}$, 0.005 M NaCl electrolyte. See main text and §2.4.1 for experimental procedure.

599 4 Discussion

600 4.1 Uranyl phosphate solution speciation

601 In the present study, FTIR bands characteristics are reported for uranyl phosphate solution
602 species formed at pH 4, under conditions of low (VI) concentrations and moderate phosphate
603 ligand concentration ($[U]_{l, aq}$: 2 μ M and 10 μ M, $[P]_{l, aq}$: 100 μ M), for which $UO_2HPO_{4(aq)}$ species
604 are calculated to be predominant aqueous species by using the MINTEQA2 code. However, the
605 high (baseline corrected) IR absorbance that we observed in the present speciation study
606 suggests the precipitation of a U(VI)-phosphate phase, too (as the IR absorbance is at least two
607 orders of magnitude larger than that of the uranyl phosphate surface species formed onto NaIdP,
608 under similar conditions). Hence, the experimental solutions studied here might be unstable (in
609 the absence of NaIdP) and uranyl phosphates colloids formed directly from the solutions might
610 undergo a sedimentation onto the ATR FTIR crystal. This hypothesis is consistent with the
611 batch experiments results indicating the formation of small amounts (ca. 5% of total U) of
612 uranyl phosphate colloids at pH 4, in the absence of NaIdP. This is also in agreement with
613 saturation index calculations, which indicated that the experimental solutions (at pH 4, $[U]_{l, aq}$
614 = 10 μ M and $[P]_{l, aq}$ = 100 μ M) were over-saturated with respect to a U(VI)-phosphate mineral,
615 namely $(UO_2)_3(PO_4)_2(s)$, and slightly oversaturated with respect to Na-autunite. The IR bands
616 identified in the present study show similar positions of ν_3 P-O bands at 1122 and 993 cm^{-1} and
617 of ν_3 U=O band at 940 cm^{-1} than those reported in the literature for $(UO_2)_3(PO_4)_2 \cdot 4H_2O(s)$ ([91]).
618 The main strong band at 996 cm^{-1} and the small bands at 924 and 1122 cm^{-1} observable on the
619 FTIR spectra are consistent with those reported by Comarmond et al. [54] for U-P solution
620 species (pH 4, $[U]_{l, aq}$ = $[P]_{l, aq}$ = 20 μ M), too. These authors have reported identical IR spectral
621 features for uranyl phosphate aqueous species and U(VI) phosphate precipitates forming at
622 acidic pH. They have suggested the formation in their experiments of an aqueous uranyl
623 phosphate complex, with a monodentate complexation mode between uranyl and phosphate

624 ions based on the evidence of a C_{3v} molecular symmetry of the PO_4 unit (two ν_3 P-O), and on
625 band positions (at 1122 and 996 cm^{-1}), as well as formation of an U(VI)-phosphate mineral.
626 The main uranyl phosphate aqueous species expected in our experimental solutions at pH 4 is
627 $UO_2HPO_4(aq)$, in which the molecular symmetry of PO_4 unit is C_1 (with three ν_3 P-O bands
628 observable in IR spectra), while only two ν_3 bands were however observed in the IR spectra of
629 the U-P solutions studied. However, the contribution of a uranyl phosphate aqueous complex
630 to the IR spectra of our U-P solutions cannot be excluded. DFT calculations carried out for
631 different modes of uranyl-phosphate complexation have been reported in the literature [92].
632 The authors have indicated that hydrated UO_2HPO_4 species containing 4 structural water
633 molecules (e.g., $UO_2HPO_4(H_2O)_4$) have a ν_3 band of U=O at 940 cm^{-1} , which is close to the
634 value reported by Comarmond et al. [54] and in the present work. Interestingly, the DFT
635 calculation ([92]) carried out for a cluster of $UO_2HPO_4(H_2O)_4$ has shown the transfer of a proton
636 from water equatorially-coordinated to the uranyl ion to an oxygen atom of the phosphate ion.
637 This proton transfer was reported to lead to a diprotonated phosphate ion, i.e.,
638 $UO_2H_2PO_4(H_2O)_3OH$, with the PO_4 unit having a C_{3v} molecular symmetry. Based on the above
639 discussion, it is likely that an uranyl phosphate aqueous complex with a molecular structure like
640 $UO_2HPO_4(H_2O)_4$ (having an equivalent structure as $UO_2H_2PO_4(H_2O)_3OH$) contributed to IR
641 signals of the U-P solutions studied here. There was also observed on our IR spectra two ν_3 P-
642 O bands at 1055 and 1170 cm^{-1} . These bands may be attributed to formation of an additional
643 uranyl phosphate aqueous complex, -as it was reported that solid phases have rather small
644 band's width [54,76]-. Such additional complex possibly has a C_{2v} -like symmetry (as its ν_3
645 bands at 1052 and 1170 cm^{-1} may result from a shift of the ν_3 bands at 1075 and 1160 cm^{-1} of
646 $H_2PO_4^-$ aqueous species). A third ν_3 band of small intensity would be expected at a low
647 wavenumber (around 940 cm^{-1}) but the strong band observable at 997 cm^{-1} in our IR spectra
648 may overlap with it. The additional species is possibly $UO_2H_2PO_4^+(aq)$ which is expected to exist

649 as a minor uranyl phosphate aqueous species according to speciation calculations. If this species
650 has a C_{2v} -like symmetry, the phosphate ion should be coordinated to the uranyl ion in a bidentate
651 mode and the hydrated form of $UO_2H_2PO_4^+$ may be $UO_2H_2PO_4^+ \cdot 3H_2O$. Further studies using
652 complementary techniques like TRLFS and EXAFS may be helpful to confirm this hypothesis.

653 *4.2 Surface speciation of uranyl ions at the NaIdP-solution interface*

654 A recently published study [93] has shown the presence of two ν_3 U=O bands at 910 and 900
655 cm^{-1} on ATR FTIR spectra acquired during the sorption of uranyl ions (at $[U]_{l, aq}$: 20 μM) at
656 near-neutral pH (6.8) onto montmorillonite. The authors have suggested that the strong sorption
657 of aqueous $UO_2(OH)_2$ ions onto the clay surface led to a shift in the wavenumber of ν_3 U=O
658 band of more than 10 cm^{-1} . In the present study, the ν_3 IR bands of uranyl ions ($< 960 cm^{-1}$)
659 could not be studied. However, our U(VI) macroscopic sorption results indicated that several
660 sorption mechanisms / species can contribute to the uptake of uranyl ions by NaIdP, depending
661 on key parameters such as pH, U concentration and clay-to-solution ratio. Data presented here
662 show a decrease in the U sorption percentage, at a given acidic pH, when increasing U
663 concentration in a certain range (1-10 μM) or when decreasing the clay-to-solution ratio (from
664 3 to 1 $g.L^{-1}$). These trends strongly suggest that a very low amount of high affinity sorption sites
665 ($< 0.02 sites.nm^{-2}$) at NaIdP edge platelets, which interact strongly with U, become
666 progressively saturated while low affinity surface sites are increasingly involved in U sorption.
667 It has long been reported that 2:1 layers clay minerals display different types of surface sites
668 having distinct concentrations and affinity towards H^+ and other aqueous ions [94], including
669 silanol, aluminol and ferrinol sites at clay edges. Bradbury and Baeyens [50,89] have provided
670 modelling of trace metals and actinides sorption onto Na-illite by using a non-electrostatic
671 model, which included two-sites protolysis non-electrostatic surface complexation and cation
672 exchange. The authors could fit successfully their macroscopic data on U(VI) sorption by
673 considering a mechanism of cation exchange implying UO_2^{2+} in clay interlayer space (and

674 dominating in the pH range 2.5-3.5) and the strong sorption of U by formation of uranyl surface
675 complexes of the types $\Xi\text{SO}^s\text{UO}_2^+$, $\Xi\text{SO}^s\text{UO}_2\text{OH}$ and $\Xi\text{SO}^s\text{UO}_2\text{OH}_2^-$ that involve high affinity
676 sites (noted ΞSO^s) present in low amounts (ca. 0.01 sites. nm^{-2}) at clay edges. Several EXAFS
677 analyses have moreover provided evidence that uranyl ions are sorbed, at low pH, as
678 exchangeable UO_2^{2+} in the interlayer space of smectitic clays, and at moderately acidic pH, as
679 additional inner-sphere uranyl surface complex and / or U(VI) polynuclear surface species,
680 depending on surface coverage [13,64–66]. Uranyl carbonate ISSC were also shown to form at
681 edge sites of smectite platelets when increasing pH [67]. Based on spectroscopic results, Troyer
682 et al. [71] could fit U(VI) sorption isotherms (in the concentration range 1-10 μM) on
683 montmorillonite by using in surface complexation modeling three types of species, namely,
684 cation-exchanged UO_2^{2+} (noted UO_2X_2), a cationic surface complex (ΞSOUO_2^+) and a ternary
685 uranyl carbonate surface complex ($\Xi\text{SOUO}_2\text{CO}_3^-$), which dominated at pH 4, 6 and 8,
686 respectively. Our results are consistent with those reported in the above-mentioned modeling
687 or spectroscopic studies. They suggest a variable contribution of both high affinity and low
688 affinity surface sites to the sorption of uranyl ions onto NaIdP edges, at acidic pH, via formation
689 of ISSC of U(VI), in most of the conditions investigated. Unlike for the montmorillonite [71],
690 the relative contribution of cation-exchanged UO_2^{2+} is not observable for NaIdP, due to the
691 difference in permanent structural charge between these two types of clay. As no significant
692 effect of U(VI) sorption on EM is observable at $\text{pH} < 5$ in our experiments, even at the highest
693 U concentrations investigated, it is possible that the sorption mechanisms of U(VI) onto NaIdP
694 included the deprotonation of the protonated hydroxyl sites (ferrinol / aluminol) followed by
695 the formation of $\Xi\text{SO}^s\text{UO}_2^+$ surface complexes, and / or the formation of $\Xi\text{SO}^s\text{UO}_2\text{OH}$ surface
696 complexes on neutral hydroxyl surface sites. Dahn et al. [95] have investigated by EXAFS the
697 coordination environment of uranyl ions adsorbed onto NaIdP at pH 5 (in 0.1 M NaClO_4
698 electrolyte solution) and at low surface loading of U ($4 \mu\text{mol.g}^{-1}$) and have suggested a

699 preferential binding of uranyl ions to the iron octahedral surface sites over the aluminum
700 octahedral surface sites of the clay. No evidence on the contribution to U sorption of each type
701 of surface hydroxyl at Na-illite edges can be provided in the present study. At the highest U
702 concentration values studied (25 μM), we observed an increase in the U sorption percentage
703 (and a nonlinear increase of amount of U sorbed) which is attributable to the contribution of an
704 additional sorption mechanism, likely the (surface) precipitation of a uranyl hydroxide phase.
705 Such a mechanism is possible as the sorption on low affinity edge sites of a high U concentration
706 ($> 10 \mu\text{M}$) may be less efficient to compete against the direct precipitation of a uranyl hydroxide
707 from solution. We can alternately propose the formation of surface precipitates of uranyl
708 (hydr)oxides and / or polynuclear uranyl surface species similar to those described by Sylwester
709 et al. [64], which may nucleate on clay surface, even before all weak sorption sites available for
710 U surface complexation become saturated.

711 *4.3 Surface speciation of uranyl ions at the NaIdP--phosphate-solution interface*

712 Uranyl sorption edges and isotherms presented here show that the presence of phosphate ligands
713 (100 μM) promoted U(VI) sorption at acid pH onto NaIdP, especially at a high U concentration
714 (10 μM). Moreover, phosphate ion sorption was enhanced by an increase of U concentration in
715 experiment, too. Such a phosphate signature on U(VI) sorption at a clay surface has already
716 been reported in the case of kaolinite but it was not observed for montmorillonite [71], for
717 which formation of inner-sphere surface complex (ISSC) of uranyl phosphate (with U-bridging
718 at the surface) was reported. Macroscopic results given in the present study suggest thus a strong
719 involvement of phosphate ligands in U(VI) surface speciation in NaIdP – phosphate – solution
720 systems, with (great part of) uranyl ions sorbed via formation of uranyl phosphate ternary
721 surface complex(es) and/or U(VI) phosphate surface precipitates. Experimental results, such as
722 the non-linear increase of U and P surface coverages when increasing U concentration (from 1
723 to 10 μM), highlighted moreover the formation of multiple uranyl phosphate sorption species

724 and/or the implications of several types of surface sites. Desorption experiments provided
725 strong evidence that the sorption of U at acidic pH has occurred in the presence of phosphate
726 ions mainly via a reversible process, i.e., via uranyl phosphate surface complex formation.
727 Formation of such surface complexes were shown to impart negative charges to the clay surface
728 throughout the pH range investigated, which is an additional indication of the participation of
729 phosphate anions. Based on values of high-affinity sites given in literature [50] for the
730 conditioned Illite du Puy (ca. $2 \mu\text{mol.g}^{-1}$ or $0.01 \text{ sites.nm}^{-2}$), it is likely that uranyl phosphate
731 surface complexes that were formed in our experiments for the moderate U and P concentrations
732 studied ($12 \mu\text{M}$ and $100 \mu\text{M}$, respectively) would involve both high- and low-affinity
733 (amphoteric) sites at clay edge platelets. The contribution of a mechanism of uranyl phosphate
734 precipitation from oversaturated solutions is not to be ruled out at the highest U concentration
735 studied, in the presence of phosphate ligands ($[\text{U}]_{\text{I,aq}} = 25 \mu\text{M}$, $R_{\text{S/L}} = 3 \text{ g.L}^{-1} \text{ NaIdP}$).

736 Our in situ ATR FTIR experiments of the U – P (co)sorption onto NaIdP conducted at varying
737 U concentration or as a function of reaction time provided valuable information on surface
738 speciation. It was found that several species contributed to the phosphate surface speciation
739 during U-P co-sorption, with three types of uranyl phosphate surface species being identified.
740 At short reaction times ($< 7 \text{ h}$), two uranyl phosphate species were identified onto NaIdP, with
741 the first one (U-P species A) being formed at low U concentration and the second one (U-P
742 species B) growing with an increase in U concentration. It should be noted that, when phosphate
743 ions were added before U in experiment, the formation of these two U-P species (and / or one
744 of the two U-P species) affected the IR signals of previously-formed phosphate surface species,
745 i.e., it led to disappearance of IR bands of preexisting ISSC of phosphate (a shift from a band
746 at 1038 cm^{-1} , attributable to an ISSC of phosphate [1], to ca. 1050 cm^{-1}). There was also
747 observed a small decrease in bands' intensity of the OSSC of phosphate. Thus, pre-existing
748 phosphate surface species formed onto NaIdP were desorbed and / or converted rapidly upon

749 the addition of uranyl ions in the system and the subsequent rapid formation of U-P surface
750 species, which are therefore interpreted as being inner sphere uranyl phosphate surface species
751 forming at edge sites of the clay platelets and competing against the existence of ISSC of
752 phosphate on illite surface. Formation of uranyl-phosphate ISSC onto NaIdP is in good
753 agreement with previously published spectroscopic studies of the (co)sorption, under conditions
754 close to those used in the present study, of uranyl and phosphate ions at surfaces of aluminum
755 / iron (hydr)oxide, SiO₂ and clays [55,54,71,59]. Regarding the uranyl phosphate surface
756 species identified in the present study, U-P species A has a (weak) IR band at ~1125 cm⁻¹, which
757 is independent of the U concentration (2–10 μM). This suggests that its formation took place at
758 high-affinity sites existing in limited amounts onto clay edges. Whether this species represents
759 a surface precipitate (e.g., (UO₂)₃(PO₄)₂·4H₂O_(s)) and / or an outer sphere surface complex (i.e.,
760 UO₂HPO₄(H₂O)₄) having a band at 1122 cm⁻¹, can be ruled out. In such cases, its absorbance
761 would increase with U concentration [96]. It is likely that this U-P species is a U-bridging ISSC
762 of uranyl phosphate because it forms onto high-affinity sites at illite platelet edges, which are
763 expected to interact strongly with U [89]. Conversely, U-P species B displays an IR band at
764 ~1050 cm⁻¹ whose intensity increases with U concentration in the range 2–8 μM, and it
765 dominates phosphate speciation at low reaction times (7 hours). Actually, this band can hardly
766 be attributed to an OSSC of uranyl phosphate (having IR bands at positions close to those of
767 aqueous UO₂H₂PO₄^{+(aq)} species), because an OSSC complex would display two bands at 1052
768 and 1170 cm⁻¹ of similar intensities (see discussion in §4.1). A reduction of molecular symmetry
769 of PO₄ unit from C_{2v} to C₁ is expected if the uranyl phosphate aqueous species is involved in
770 formation of the ternary surface complex. The band at 1050 cm⁻¹ is therefore ascribed to a
771 uranyl phosphato ISSC forming at low affinity sites onto clay edges. It should be noted that
772 formation, at a short reaction time (t_R = 7 h) during our ATR FTIR (co)sorption experiments,
773 of the two types of U-P inner sphere surface complexes has prevented the formation of (VI)-

774 phosphate colloids, which were observed in the absence of clay and under similar solution
775 conditions (see discussion in §4.1).

776 At a long reaction time (3 days) and high U concentration ($[U]_{I,aq} = 8 \mu\text{M}$), two uranyl phosphate
777 species were identified to exist onto NaIdP, namely, the U-P species B (whose formation took
778 place within the first hours and increased then slowly with time) and another species (U-P
779 species C) whose intensity was increasing with reaction time, from a reaction of ca. 5h to 3
780 days. The latter uranyl-phosphate surface species has three ν_3 P-O antisymmetric stretching
781 band at 1114, 1080 and 992 cm^{-1} , which indicates a C_{2v} or lower molecular symmetry (likely
782 C_1) of PO_4 unit. The band at 992 cm^{-1} was not observed at short reaction time ($t_R = 7\text{h}$), possibly
783 due to some interferences of IR absorption from clay structure at wavenumbers lower than 1000
784 cm^{-1} . The bands' positions of U-P species C are quite different than those observed on IR spectra
785 of uranyl phosphate solutions, ruling out formation of uranyl phosphate OSSC and / or U(VI)
786 phosphate colloids formed directly from solution. These positions are shifted with respect to
787 those reported in the literature for the group of autunite minerals but they compare well with
788 them (1118, 1074 and 985 cm^{-1} for autunite, and 1118, 1048 and 985 cm^{-1} for meta-autunite
789 [97]). Hence, we hypothesize that U-P species C is an autunite-like surface species. Formation
790 of this species may contribute to the slight increase of macroscopic P sorption on NaIdP with
791 increasing U concentration. Troyer et al. [71] have investigated by EXAFS and TRLS the
792 effect of increasing concentrations of phosphate and uranyl ions (0.025-100 μM) on the uptake
793 of U(VI) by montmorillonite at pH 4-6. These authors have evidenced a transition between
794 formation of uranyl phosphate surface complexes at low coverage of the clay, and surface
795 precipitates of U(VI)-phosphates at high surface coverage. If the U-P species C represents a
796 U(VI) phosphate precipitate formed on NaIdP, this would imply that its formation has occurred
797 in limited amounts under our experimental conditions (despite the dominance of its signal on
798 the IR spectra), because our desorption data indicate primarily reversible co-sorption

799 mechanisms. Alternately, the U-P species C can rather be an autunite-like uranyl phosphate
800 surface complex (e.g., as a polynuclear complex) that forms on NaIdP at a high reaction time.

801 It should be noticed that the successive addition of phosphate ions followed by uranyl ions, or
802 their simultaneous addition, to the NaIdP – solution system does not lead to the same surface
803 speciation, even at low reactions times (7h). The initial addition of P alone -allowing the clay
804 surface to be covered by P sorbed for the first 2h- and subsequent, progressive additions of U
805 led to the existence onto NaIdP, after a reaction time of 7h, of a (U bridging) ternary U-P
806 surface complex formed rapidly on the high-affinity clay edge sites, a U-P surface complex
807 formed progressively on the low-affinity clay edge sites, and an OSSC of phosphate (shown in
808 a previous study to transform slowly into an ISSC of phosphate, in the absence of U [1]). Instead,
809 the simultaneous addition of P and relatively high concentration of U (10 μM) resulted in the
810 existence onto NaIdP, after a reaction time of 7h, of the two former species and an autunite-like
811 surface complex/precipitate. This suggests that the formation of the U-P surface complex on
812 low-affinity sites on the clay edges is not fast enough to prevent fairly rapid nucleation of
813 surface precipitates and/or formation of polynuclear surface species of uranyl phosphate. It is
814 possible that the U-P surface complex existing on low-affinity sites is formed by the binding of
815 P on low-affinity sites (upon slow conversion of OSSC to ISSC of phosphate formed over time
816 by surface ligand exchange) and the binding of uranyl ions on sorbed P (P-bridging uranyl
817 phosphate complex). The conversion of OSSC to ISSC of phosphate, in the absence of U, was
818 found to proceed slowly up to a reaction time of 3 days, leading to the predominance of ISSC
819 of phosphate at a long reaction time, and a very intense band at 1035 cm^{-1} on the spectra of the
820 NaIdP-phosphate – solution interface. In similar conditions, with the exception of the presence
821 of $10\text{ }\mu\text{M}$ of U in the system, a (less intense) band shifted to 1050 cm^{-1} is present on the FTIR
822 interface spectra. Presumably, the formation of precipitate / polynuclear species of uranyl
823 phosphate on the clay surface limited the formation of ISSC of phosphate in the long term (and

824 presumably it also limited the amount of U-P surface complex likely to form at weak sites).
825 Formation of P-bridging uranyl phosphate surface complex on low affinity sites, and U-P
826 surface precipitates / polynuclear surface species, could explain the signature of P on the
827 macroscopic sorption of U onto NaIdP, in contrast to montmorillonite for which the existence
828 of a U-bridging uranyl phosphate ISSC has been reported [71]. The use of other spectroscopy
829 techniques is however necessary to confirm the hypothesis of a P-bridging uranyl phosphate
830 surface complex.

831 **5 Conclusions**

832 To our best knowledge, the present study is the first one combining macroscopic experiments
833 and in situ ATR FTIR spectroscopic study to investigate the (co)sorption mechanisms of
834 phosphate ions and trace levels of uranyl ions at the illite–electrolyte solution interface.

835 All the macroscopic data reported here pointed at several sorption mechanisms / surface sites
836 contributing to the uptake of uranyl ions by NaIdP and depending on key parameters such as
837 pH, U concentration, clay-to-solution ratio and phosphate ligand concentration. In peculiar, data
838 indicated that a low amount of high-affinity sorption sites (<0.02 sites.nm⁻²) existing at the
839 NaIdP edge platelets can strongly interact with U and become progressively saturated, while
840 low affinity surface sites are increasingly involved in U sorption, when increasing U
841 concentration (1-10 μ M) or decreasing clay-to-solution ratio (1-3 g.L⁻¹) in experiment. It was
842 also shown that the presence of phosphate ligands enhances the sorption of U(VI) at acidic pH
843 onto NaIdP and, conversely, the uptake of phosphate ions by the clay surface is promoted by
844 an increase of U concentration in sorption experiment. Macroscopic and EM data highlighted
845 the formation of several types of uranyl phosphate species imparting negative charges to the
846 clay surface and / or several types of sorption sites, with the mechanisms of U-P co-sorption
847 remaining highly reversible. Data acquired by in situ monitoring of the illite-solution interface
848 by ATR FTIR spectroscopy provided evidence that uranyl ions and phosphate ions were

849 (co)sorbed at acidic pH mainly via the formation of three types of inner-sphere uranyl phosphate
850 surface complexes, whose predominance depend on reaction time and U surface concentration.
851 A uranyl phosphate surface species (with a weak $\nu_3(\text{P-O})$ band at $\sim 1125 \text{ cm}^{-1}$) is formed rapidly,
852 likely at high-affinity surface sites existing in limited amounts on the clay edges, and is
853 identified as an inner sphere uranyl phosphate surface complex (possibly with a U-bridging
854 structure). An additional U-P surface complex (with a band at $\sim 1050 \text{ cm}^{-1}$) is progressively
855 formed in increasing amounts with U concentration and reaction time, likely on low affinity
856 clay edge sites. It is possible that this surface species is formed via binding of U to phosphate
857 sorbed as an inner sphere phosphate surface complex onto illite (P-bridging structure), which
858 was shown to exist on NaIdP in the absence of U [1]. Finally, an “autunite-like” uranyl
859 phosphate surface species (e.g., such as a polynuclear complex) having $\nu_3(\text{P-O})$ bands at 1114,
860 1080 and 992 cm^{-1} appears after a few hours after simultaneous addition of P and U at relatively
861 high concentration ($10 \mu\text{M}$). The present work clearly demonstrates that uranyl ions are not
862 sorbed onto illite at the expense of phosphate ion sorption but that several types of uranyl
863 phosphate sorption species are formed in NaIdP – U(VI) – phosphate – solution systems, which
864 is consistent with macroscopic data showing a strong P sorption onto illite [1], a promotion of
865 P sorption with U concentration and a signature of P on the sorption of U(VI) (this study).

866 The information on uranyl surface speciation in the presence of phosphate ligands that is
867 presented here is novel, and provides for the first time in situ spectroscopic evidence of the
868 synergistic formation of several types of uranyl phosphate sorption species on the surface of a
869 2:1 layered clay, namely illite, which is an important phase in soils and clay formations. This
870 knowledge is important to better understand / predict the effect of clay surface property and its
871 impact on the sorption behavior of uranyl and phosphate ions in the environment and / or to
872 model the long-term behavior of U(VI) in argillaceous formations where illite is the main clay

873 constituent, such as those envisaged as barriers to U dissemination in the far-field of HLW deep
874 repository.

875 .

876 **Acknowledgments**

877 We thank for analyses of clay samples: ITES (Institut Terre et Environnement de Strasbourg,
878 Strasbourg University, France) for mineralogical analyses, SARM-CRPG (Service d'Analyse
879 des Roches et Minéraux, Centre de Recherches Pétrographiques et Géochimiques, Nancy,
880 France) for major element and trace element analysis, and ECPM (École de Chimie des
881 Polymères et Matériaux, Strasbourg, France) for BET measurements. We are grateful to the A.
882 Boos for giving us access to the ICP-OES and ICP-MS equipments of the "Plateforme des
883 Inorganiques" of IPHC for our solution analyses. We are very grateful to an anonymous
884 reviewer and to the Editor, Professor Robert Tilton, for their constructive comments, which
885 improved the manuscript considerably.

886

887 **Funding**

888 This research work was funded by the European Commission in the frame of the European Joint
889 Programme on Radioactive Waste Management EURAD (Grant agreement ID 847593, contract
890 number CNRS 198255) and took place in the Work Package FUTURE of EURAD.

891 **Appendix A. Supporting Information**

892

- 894 [1] S.Y. Guo, M. Del Nero, O. Courson, S. Meyer-Georg, R. Barillon, Speciation studies at
895 the Illite - solution interface: Part 1 – Sorption of phosphate ions, *Colloids and Surfaces*
896 *A: Physicochemical and Engineering Aspects.* 682 (2024) 132905.
897 <https://doi.org/10.1016/j.colsurfa.2023.132905>.
- 898 [2] S.J. Morrison, L.S. Cahn, Mineralogical residence of alpha-emitting contamination and
899 implications for mobilization from uranium mill tailings, *Journal of Contaminant*
900 *Hydrology.* 8 (1991) 1–21. [https://doi.org/10.1016/0169-7722\(91\)90006-M](https://doi.org/10.1016/0169-7722(91)90006-M).
- 901 [3] R.G. Riley, J.M. Zachara, F.J. Wobber, Chemical Contaminants on DOE Lands and
902 Selection of Contaminant Mixtures for Subsurface Science Research, DOE/ER-0547T.
903 U.S. Department of Energy. (1992).
- 904 [4] W.-M. Wu, J. Carley, M. Fienen, T. Mehlhorn, K. Lowe, J. Nyman, J. Luo, M.E. Gentile,
905 R. Rajan, D. Wagner, R.F. Hickey, B. Gu, D. Watson, O.A. Cirpka, P.K. Kitanidis, P.M.
906 Jardine, C.S. Criddle, Pilot-Scale in Situ Bioremediation of Uranium in a Highly
907 Contaminated Aquifer. 1. Conditioning of a Treatment Zone, *Environ. Sci. Technol.* 40
908 (2006) 3978–3985. <https://doi.org/10.1021/es051954y>.
- 909 [5] K. Maher, J.R. Bargar, G.E. Brown, Environmental Speciation of Actinides, *Inorg. Chem.*
910 52 (2013) 3510–3532. <https://doi.org/10.1021/ic301686d>.
- 911 [6] S.A. Cumberland, G. Douglas, K. Grice, J.W. Moreau, Uranium mobility in organic
912 matter-rich sediments: A review of geological and geochemical processes, *Earth-Science*
913 *Reviews.* 159 (2016) 160–185. <https://doi.org/10.1016/j.earscirev.2016.05.010>.
- 914 [7] R.C. Ewing, R.A. Whittleston, B.W.D. Yardley, Geological Disposal of Nuclear Waste: a
915 Primer, *ELEMENTS.* 12 (2016) 233–237. <https://doi.org/10.2113/gselements.12.4.233>.
- 916 [8] S.V. Churakov, W. Hummel, M.M. Fernandes, Fundamental Research on Radiochemistry
917 of Geological Nuclear Waste Disposal, *Chimia.* 74 (2020) 1000.
918 <https://doi.org/10.2533/chimia.2020.1000>.
- 919 [9] T.A. Kurniawan, M.H.D. Othman, D. Singh, R. Avtar, G.H. Hwang, T. Setiadi, W. Lo,
920 Technological solutions for long-term storage of partially used nuclear waste: A critical
921 review, *Annals of Nuclear Energy.* 166 (2022) 108736.
922 <https://doi.org/10.1016/j.anucene.2021.108736>.
- 923 [10] B. Grambow, Geological Disposal of Radioactive Waste in Clay, *ELEMENTS.* 12 (2016)
924 239–245. <https://doi.org/10.2113/gselements.12.4.239>.
- 925 [11] G. Montavon, S. Ribet, Y.H. Loni, F. Maia, C. Bailly, K. David, C. Lerouge, B. Madé,
926 J.C. Robinet, B. Grambow, Uranium retention in a Callovo-Oxfordian clay rock formation:
927 From laboratory-based models to in natura conditions, *Chemosphere.* 299 (2022) 134307.
928 <https://doi.org/10.1016/j.chemosphere.2022.134307>.
- 929 [12] P. Krejci, T. Gimmi, L.R. Van Loon, On the concentration-dependent diffusion of sorbed
930 cesium in Opalinus Clay, *Geochimica et Cosmochimica Acta.* 298 (2021) 149–166.
931 <https://doi.org/10.1016/j.gca.2021.01.012>.
- 932 [13] M. Marques Fernandes, B. Baeyens, R. Dähn, A.C. Scheinost, M.H. Bradbury, U(VI)
933 sorption on montmorillonite in the absence and presence of carbonate: A macroscopic and
934 microscopic study, *Geochimica et Cosmochimica Acta.* 93 (2012) 262–277.
935 <https://doi.org/10.1016/j.gca.2012.04.017>.
- 936 [14] V. Montoya, B. Baeyens, M.A. Glaus, T. Kupcik, M. Marques Fernandes, L. Van Laer, C.
937 Bruggeman, N. Maes, T. Schäfer, Sorption of Sr, Co and Zn on illite: Batch experiments
938 and modelling including Co in-diffusion measurements on compacted samples,
939 *Geochimica et Cosmochimica Acta.* 223 (2018) 1–20.
940 <https://doi.org/10.1016/j.gca.2017.11.027>.
- 941 [15] C. Tournassat, R.M. Tinnacher, S. Grangeon, J.A. Davis, Modeling uranium(VI)
942 adsorption onto montmorillonite under varying carbonate concentrations: A surface

- 943 complexation model accounting for the spillover effect on surface potential, *Geochimica*
944 *et Cosmochimica Acta*. 220 (2018) 291–308. <https://doi.org/10.1016/j.gca.2017.09.049>.
- 945 [16] B. Ma, L. Charlet, A. Fernandez-Martinez, M. Kang, B. Madé, A review of the retention
946 mechanisms of redox-sensitive radionuclides in multi-barrier systems, *Applied*
947 *Geochemistry*. 100 (2019) 414–431. <https://doi.org/10.1016/j.apgeochem.2018.12.001>.
- 948 [17] G.R. Choppin, Soluble rare earth and actinide species in seawater, *Marine Chemistry*. 28
949 (1989) 19–26. [https://doi.org/10.1016/0304-4203\(89\)90184-9](https://doi.org/10.1016/0304-4203(89)90184-9).
- 950 [18] I. Grenthe, J. Fuger, R.J. Lemire, A.B. Muller, C. Nguyen-Trung Cregu, H. Wanner,
951 Chemical thermodynamics of uranium, Elsevier Science Publishers, Netherlands, 1992.
- 952 [19] V. Eliet, G. Bidoglio, N. Omenetto, L. Parma, I. Grenthe, Characterisation of hydroxide
953 complexes of uranium(VI) by time-resolved fluorescence spectroscopy, *Faraday Trans.*
954 91 (1995) 2275. <https://doi.org/10.1039/ft9959102275>.
- 955 [20] R.J. Silva, H. Nitsche, Actinide Environmental Chemistry:, *Radiochimica Acta*. 70–71
956 (1995) 377–396. <https://doi.org/10.1524/ract.1995.7071.s1.377>.
- 957 [21] S. Pompe, K. Schmeide, M. Bubner, G. Geipel, K.H. Heise, G. Bernhard, H. Nitsche,
958 Investigation of humic acid complexation behavior with uranyl ions using modified
959 synthetic and natural humic acids:, *Radiochimica Acta*. 88 (2000) 553–558.
960 <https://doi.org/10.1524/ract.2000.88.9-11.553>.
- 961 [22] A. Sandino, J. Bruno, The solubility of $(\text{UO}_2)_3(\text{PO}_4)_2 \cdot 4\text{H}_2\text{O}(\text{s})$ and the formation of U(VI)
962 phosphate complexes: Their influence in uranium speciation in natural waters,
963 *Geochimica et Cosmochimica Acta*. 56 (1992) 4135–4145. [https://doi.org/10.1016/0016-7037\(92\)90256-I](https://doi.org/10.1016/0016-7037(92)90256-I).
- 964 [23] D. Gorman-Lewis, P.C. Burns, J.B. Fein, Review of uranyl mineral solubility
965 measurements, *The Journal of Chemical Thermodynamics*. 40 (2008) 335–352.
966 <https://doi.org/10.1016/j.jct.2007.12.004>.
- 967 [24] W. Um, Z. Wang, R.J. Serne, B.D. Williams, C.F. Brown, C.J. Dodge, A.J. Francis,
968 Uranium Phases in Contaminated Sediments below Hanford’s U Tank Farm, *Environ. Sci.*
969 *Technol.* 43 (2009) 4280–4286. <https://doi.org/10.1021/es900203r>.
- 970 [25] D. Gorman-Lewis, T. Shvareva, K.-A. Kubatko, P.C. Burns, D.M. Wellman, B.
971 McNamara, J.E.S. Szymanowski, A. Navrotsky, J.B. Fein, Thermodynamic Properties of
972 Autunite, Uranyl Hydrogen Phosphate, and Uranyl Orthophosphate from Solubility and
973 Calorimetric Measurements, *Environ. Sci. Technol.* 43 (2009) 7416–7422.
974 <https://doi.org/10.1021/es9012933>.
- 975 [26] M.F. Fanizza, H. Yoon, C. Zhang, M. Oostrom, T.W. Wietsma, N.J. Hess, M.E. Bowden,
976 T.J. Strathmann, K.T. Finneran, C.J. Werth, Pore-scale evaluation of uranyl phosphate
977 precipitation in a model groundwater system, *Water Resources Research*. 49 (2013) 874–
978 890. <https://doi.org/10.1002/wrcr.20088>.
- 979 [27] V.S. Mehta, F. Maillot, Z. Wang, J.G. Catalano, D.E. Giammar, Effect of co-solutes on
980 the products and solubility of uranium(VI) precipitated with phosphate, *Chemical*
981 *Geology*. 364 (2014) 66–75. <https://doi.org/10.1016/j.chemgeo.2013.12.002>.
- 982 [28] M. Kanematsu, N. Perdrial, W. Um, J. Chorover, P.A. O’Day, Influence of Phosphate and
983 Silica on U(VI) Precipitation from Acidic and Neutralized Wastewaters, *Environ. Sci.*
984 *Technol.* 48 (2014) 6097–6106. <https://doi.org/10.1021/es4056559>.
- 985 [29] D.E. Morris, P.G. Allen, J.M. Berg, C.J. Chisholm-Brause, S.D. Conradson, R.J. Donohoe,
986 N.J. Hess, J.A. Musgrave, C.D. Tait, Speciation of Uranium in Fernald Soils by Molecular
987 Spectroscopic Methods: Characterization of Untreated Soils, *Environ. Sci. Technol.* 30
988 (1996) 2322–2331. <https://doi.org/10.1021/es950745i>.
- 989 [30] T. Murakami, T. Ohnuki, H. Isobe, T. Sato, Mobility of uranium during weathering,
990 *American Mineralogist*. 82 (1997) 888–899. <https://doi.org/10.2138/am-1997-9-1006>.
- 991

- 992 [31] R. Finch, T. Murakami, 3. Systematics and Paragenesis of Uranium Minerals, in: P.C.
993 Burns, R.J. Finch (Eds.), Uranium, De Gruyter, 1999: pp. 91–180.
994 <https://doi.org/10.1515/9781501509193-008>.
- 995 [32] J.L. Jerden, A.K. Sinha, L. Zelazny, Natural immobilization of uranium by phosphate
996 mineralization in an oxidizing saprolite–soil profile: chemical weathering of the Coles Hill
997 uranium deposit, Virginia, *Chemical Geology*. 199 (2003) 129–157.
998 [https://doi.org/10.1016/S0009-2541\(03\)00080-9](https://doi.org/10.1016/S0009-2541(03)00080-9).
- 999 [33] J.G. Catalano, J.P. McKinley, J.M. Zachara, S.M. Heald, S.C. Smith, G.E. Brown,
1000 Changes in Uranium Speciation through a Depth Sequence of Contaminated Hanford
1001 Sediments, *Environ. Sci. Technol.* 40 (2006) 2517–2524.
1002 <https://doi.org/10.1021/es0520969>.
- 1003 [34] J.L. Jerden, A.K. Sinha, Geochemical coupling of uranium and phosphorous in soils
1004 overlying an unmined uranium deposit: Coles Hill, Virginia, *Journal of Geochemical*
1005 *Exploration*. 91 (2006) 56–70. <https://doi.org/10.1016/j.gexplo.2005.12.003>.
- 1006 [35] Y. Arai, D.L. Sparks, Phosphate Reaction Dynamics in Soils and Soil Components: A
1007 Multiscale Approach, in: *Advances in Agronomy*, Elsevier, 2007: pp. 135–179.
1008 [https://doi.org/10.1016/S0065-2113\(06\)94003-6](https://doi.org/10.1016/S0065-2113(06)94003-6).
- 1009 [36] D.M. Singer, J.M. Zachara, G.E. Brown Jr, Uranium Speciation As a Function of Depth
1010 in Contaminated Hanford Sediments - A Micro-XRF, Micro-XRD, and Micro- And Bulk-
1011 XAFS Study, *Environ. Sci. Technol.* 43 (2009) 630–636.
1012 <https://doi.org/10.1021/es8021045>.
- 1013 [37] J.E. Stubbs, L.A. Veblen, D.C. Elbert, J.M. Zachara, J.A. Davis, D.R. Veblen, Newly
1014 recognized hosts for uranium in the Hanford Site vadose zone, *Geochimica et*
1015 *Cosmochimica Acta*. 73 (2009) 1563–1576. <https://doi.org/10.1016/j.gca.2008.12.004>.
- 1016 [38] A.J. Pinto, M.A. Gonçalves, C. Prazeres, J.M. Astilleros, M.J. Batista, Mineral
1017 replacement reactions in naturally occurring hydrated uranyl phosphates from the Tarabau
1018 deposit: Examples in the Cu–Ba uranyl phosphate system, *Chemical Geology*. 312–313
1019 (2012) 18–26. <https://doi.org/10.1016/j.chemgeo.2012.04.004>.
- 1020 [39] J. Bruno, J. De Pablo, L. Duro, E. Figuerola, Experimental study and modeling of the
1021 U(VI)-Fe(OH)₃ surface precipitation/coprecipitation equilibria, *Geochimica et*
1022 *Cosmochimica Acta*. 59 (1995) 4113–4123. [https://doi.org/10.1016/0016-](https://doi.org/10.1016/0016-7037(95)00243-S)
1023 [7037\(95\)00243-S](https://doi.org/10.1016/0016-7037(95)00243-S).
- 1024 [40] M. Del Nero, S. Salah, T. Miura, A. Clément, F. Gauthier-Lafaye, Sorption/Desorption
1025 Processes of Uranium in Clayey Samples of the Bangombe Natural Reactor Zone, Gabon,
1026 *Radiochimica Acta*. 87 (1999) 135–150. <https://doi.org/10.1524/ract.1999.87.34.135>.
- 1027 [41] M.M.S. Cabral Pinto, M.M.V.G. Silva, A.M.R. Neiva, Release, Migration, Sorption and
1028 (re)precipitation of U During a Granite Alteration under Oxidizing Conditions, *Procedia*
1029 *Earth and Planetary Science*. 8 (2014) 28–32.
1030 <https://doi.org/10.1016/j.proeps.2014.05.007>.
- 1031 [42] M. Edahbi, B. Plante, M. Benzaazoua, M. Ward, M. Pelletier, Mobility of rare earth
1032 elements in mine drainage: Influence of iron oxides, carbonates, and phosphates,
1033 *Chemosphere*. 199 (2018) 647–654. <https://doi.org/10.1016/j.chemosphere.2018.02.054>.
- 1034 [43] M. Del Nero, A. Froideval, C. Gaillard, G. Mignot, R. Barillon, I. Munier, A. Ozgümüs,
1035 Mechanisms of uranyl sorption, Geological Society, London, Special Publications. 236
1036 (2004) 545–560. <https://doi.org/10.1144/GSL.SP.2004.236.01.30>.
- 1037 [44] S. Salah, F. Gauthier-Lafaye, M. Del Nero, G. Le Bricon, G. Bracke, Behavior of REE in
1038 the Weathering Sequence of the Natural Fission Reactor at Bangombe (Oklo)., In: *Abstr.*
1039 *of the Int. Conf. European Union of Geosciences EUG 10*, Strasbourg, France,. (1999).
- 1040 [45] T.E. Payne, G.R. Lumpkin, T.D. Waite, Chapter 2 - UraniumVI Adsorption on Model
1041 Minerals: Controlling Factors and Surface Complexation Modeling, in: E.A. Jenne (Ed.),

- 1042 Adsorption of Metals by Geomedia, Academic Press, San Diego, 1998: pp. 75–97.
1043 <https://doi.org/10.1016/B978-012384245-9/50003-7>.
- 1044 [46] Z. Guo, C. Yan, J. Xu, W. Wu, Sorption of U(VI) and phosphate on γ -alumina: Binary
1045 and ternary sorption systems, *Colloids and Surfaces A: Physicochemical and Engineering*
1046 *Aspects*. 336 (2009) 123–129. <https://doi.org/10.1016/j.colsurfa.2008.11.032>.
- 1047 [47] Z. Guo, Y. Li, W. Wu, Sorption of U(VI) on goethite: Effects of pH, ionic strength,
1048 phosphate, carbonate and fulvic acid, *Applied Radiation and Isotopes*. 67 (2009) 996–
1049 1000. <https://doi.org/10.1016/j.apradiso.2009.02.001>.
- 1050 [48] T. Hiemstra, W.H.V. Riemsdijk, A. Rossberg, K.-U. Ulrich, A surface structural model
1051 for ferrihydrite II: Adsorption of uranyl and carbonate, *Geochimica et Cosmochimica Acta*.
1052 73 (2009) 4437–4451. <https://doi.org/10.1016/j.gca.2009.04.035>.
- 1053 [49] G.D. Turner, J.M. Zachara, J.P. Mckinley, S.C. Smith, Surface-charge properties and UO
1054 z' adsorption of a subsurface smectite, (1996). [https://doi.org/10.1016/0016-](https://doi.org/10.1016/0016-7037(96)00169-X)
1055 [7037\(96\)00169-X](https://doi.org/10.1016/0016-7037(96)00169-X).
- 1056 [50] M.H. Bradbury, B. Baeyens, Sorption modelling on illite Part I: Titration measurements
1057 and the sorption of Ni, Co, Eu and Sn, *Geochimica et Cosmochimica Acta*. 73 (2009) 990–
1058 1003. <https://doi.org/10.1016/j.gca.2008.11.017>.
- 1059 [51] M. Marques Fernandes, A.C. Scheinost, B. Baeyens, Sorption of trivalent lanthanides and
1060 actinides onto montmorillonite: Macroscopic, thermodynamic and structural evidence for
1061 ternary hydroxo and carbonate surface complexes on multiple sorption sites, *Water*
1062 *Research*. 99 (2016) 74–82. <https://doi.org/10.1016/j.watres.2016.04.046>.
- 1063 [52] C. Joseph, M. Stockmann, K. Schmeide, S. Sachs, V. Brendler, G. Bernhard, Sorption of
1064 U(VI) onto Opalinus Clay: Effects of pH and humic acid, *Applied Geochemistry*. 36 (2013)
1065 104–117. <https://doi.org/10.1016/j.apgeochem.2013.06.016>.
- 1066 [53] M. Stockmann, K. Fritsch, F. Bok, M.M. Fernandes, B. Baeyens, R. Steudtner, K. Müller,
1067 C. Nebelung, V. Brendler, T. Stumpf, K. Schmeide, New insights into U(VI) sorption onto
1068 montmorillonite from batch sorption and spectroscopic studies at increased ionic strength,
1069 *Science of The Total Environment*. 806 (2022) 150653.
1070 <https://doi.org/10.1016/j.scitotenv.2021.150653>.
- 1071 [54] M.J. Comarmond, R. Steudtner, M. Stockmann, K. Heim, K. Müller, V. Brendler, T.E.
1072 Payne, H. Foerstendorf, The Sorption Processes of U(VI) onto SiO₂ in the Presence of
1073 Phosphate: from Binary Surface Species to Precipitation, *Environ. Sci. Technol.* 50 (2016)
1074 11610–11618. <https://doi.org/10.1021/acs.est.6b02075>.
- 1075 [55] C. Galindo, M.D. Nero, R. Barillon, E. Halter, B. Made, Mechanisms of uranyl and
1076 phosphate (co)sorption: Complexation and precipitation at α -Al₂O₃ surfaces, *Journal of*
1077 *Colloid and Interface Science*. 347 (2010) 282–289.
1078 <https://doi.org/10.1016/j.jcis.2010.03.045>.
- 1079 [56] A. Singh, K.-U. Ulrich, D.E. Giammar, Impact of phosphate on U(VI) immobilization in
1080 the presence of goethite, *Geochimica et Cosmochimica Acta*. 74 (2010) 6324–6343.
1081 <https://doi.org/10.1016/j.gca.2010.08.031>.
- 1082 [57] J.R. Bargar, R. Reitmeyer, J.A. Davis, Spectroscopic Confirmation of
1083 Uranium(VI)–Carbonato Adsorption Complexes on Hematite, *Environ. Sci. Technol.* 33
1084 (1999) 2481–2484. <https://doi.org/10.1021/es990048g>.
- 1085 [58] J.R. Bargar, R. Reitmeyer, J.J. Lenhart, J.A. Davis, Characterization of U(VI)-carbonato
1086 ternary complexes on hematite: EXAFS and electrophoretic mobility measurements,
1087 *Geochimica et Cosmochimica Acta*. 64 (2000) 2737–2749.
1088 [https://doi.org/10.1016/S0016-7037\(00\)00398-7](https://doi.org/10.1016/S0016-7037(00)00398-7).
- 1089 [59] A. Singh, J.G. Catalano, K.-U. Ulrich, D.E. Giammar, Molecular-Scale Structure of
1090 Uranium(VI) Immobilized with Goethite and Phosphate, *Environ. Sci. Technol.* 46 (2012)
1091 6594–6603. <https://doi.org/10.1021/es300494x>.

- 1092 [60] A. Froideval, M. Del Nero, R. Barillon, J. Hommet, G. Mignot, pH dependence of uranyl
1093 retention in a quartz/solution system: an XPS study, *Journal of Colloid and Interface*
1094 *Science*. 266 (2003) 221–235. [https://doi.org/10.1016/S0021-9797\(03\)00528-9](https://doi.org/10.1016/S0021-9797(03)00528-9).
- 1095 [61] A. Froideval, M. Del Nero, C. Gaillard, R. Barillon, I. Rossini, J.L. Hazemann, Uranyl
1096 sorption species at low coverage on Al-hydroxide: TRLFS and XAFS studies, *Geochimica*
1097 *et Cosmochimica Acta*. 70 (2006) 5270–5284. <https://doi.org/10.1016/j.gca.2006.08.027>.
- 1098 [62] K. Müller, H. Foerstendorf, V. Brendler, A. Rossberg, K. Stolze, A. Gröschel, The surface
1099 reactions of U(VI) on γ -Al₂O₃ — In situ spectroscopic evaluation of the transition from
1100 sorption complexation to surface precipitation, *Chemical Geology*. 357 (2013) 75–84.
1101 <https://doi.org/10.1016/j.chemgeo.2013.08.033>.
- 1102 [63] Y. Jo, J.-Y. Lee, J.-I. Yun, Adsorption of uranyl tricarbonate and calcium uranyl carbonate
1103 onto γ -alumina, *Applied Geochemistry*. 94 (2018) 28–34.
1104 <https://doi.org/10.1016/j.apgeochem.2018.05.004>.
- 1105 [64] E.R. Sylwester, E.A. Hudson, P.G. Allen, The structure of uranium (VI) sorption
1106 complexes on silica, alumina, and montmorillonite, *Geochimica et Cosmochimica Acta*.
1107 64 (2000) 2431–2438. [https://doi.org/10.1016/S0016-7037\(00\)00376-8](https://doi.org/10.1016/S0016-7037(00)00376-8).
- 1108 [65] C.J. Chisholm-Brause, J.M. Berg, R.A. Matzner, D.E. Morris, Uranium(VI) Sorption
1109 Complexes on Montmorillonite as a Function of Solution Chemistry, *Journal of Colloid*
1110 *and Interface Science*. 233 (2001) 38–49. <https://doi.org/10.1006/jcis.2000.7227>.
- 1111 [66] C. Hennig, T. Reich, R. Dähn, A.M. Scheidegger, Structure of uranium sorption
1112 complexes at montmorillonite edge sites, *Radiochimica Acta*. 90 (2002) 653–657.
1113 https://doi.org/10.1524/ract.2002.90.9-11_2002.653.
- 1114 [67] J.G. Catalano, G.E. Brown, Uranyl adsorption onto montmorillonite: Evaluation of
1115 binding sites and carbonate complexation, *Geochimica et Cosmochimica Acta*. 69 (2005)
1116 2995–3005. <https://doi.org/10.1016/j.gca.2005.01.025>.
- 1117 [68] Y. Tang, R.J. Reeder, Uranyl and arsenate cosorption on aluminum oxide surface,
1118 *Geochimica et Cosmochimica Acta*. 73 (2009) 2727–2743.
1119 <https://doi.org/10.1016/j.gca.2009.02.003>.
- 1120 [69] A. Singh, J.G. Catalano, K.-U. Ulrich, D.E. Giammar, Molecular-Scale Structure of
1121 Uranium(VI) Immobilized with Goethite and Phosphate, *Environ. Sci. Technol.* 46 (2012)
1122 6594–6603. <https://doi.org/10.1021/es300494x>.
- 1123 [70] M. Del Nero, C. Galindo, R. Barillon, B. Madé, TRLFS Evidence for Precipitation of
1124 Uranyl Phosphate on the Surface of Alumina: Environmental Implications, *Environ. Sci.*
1125 *Technol.* 45 (2011) 3982–3988. <https://doi.org/10.1021/es2000479>.
- 1126 [71] L.D. Troyer, F. Maillot, Z. Wang, Z. Wang, V.S. Mehta, D.E. Giammar, J.G. Catalano,
1127 Effect of phosphate on U(VI) sorption to montmorillonite: Ternary complexation and
1128 precipitation barriers, *Geochimica et Cosmochimica Acta*. 175 (2016) 86–99.
1129 <https://doi.org/10.1016/j.gca.2015.11.029>.
- 1130 [72] A. Gładysz-Płaska, E. Grabias, M. Majdan, Simultaneous adsorption of uranium(VI) and
1131 phosphate on red clay, *Progress in Nuclear Energy*. 104 (2018) 150–159.
1132 <https://doi.org/10.1016/j.pnucene.2017.09.010>.
- 1133 [73] M.A. Glaus, M. Aertsens, N. Maes, L. Van Laer, L.R. Van Loon, Treatment of boundary
1134 conditions in through-diffusion: A case study of ⁸⁵Sr²⁺ diffusion in compacted illite,
1135 *Journal of Contaminant Hydrology*. 177–178 (2015) 239–248.
1136 <https://doi.org/10.1016/j.jconhyd.2015.03.010>.
- 1137 [74] G.W. Brindley, G. Brown, *Crystal Structures of Clay Minerals and Their X-ray*
1138 *Identification.*, Mineralogical Society, 1980.
- 1139 [75] M.I. Tejedor-Tejedor, M.A. Anderson, The protonation of phosphate on the surface of
1140 goethite as studied by CIR-FTIR and electrophoretic mobility, *Langmuir*. 6 (1990) 602–
1141 611. <https://doi.org/10.1021/la00093a015>.

- 1142 [76] P. Persson, N. Nilsson, S. Sjöberg, Structure and Bonding of Orthophosphate Ions at the
1143 Iron Oxide–Aqueous Interface, *Journal of Colloid and Interface Science*. 177 (1996) 263–
1144 275. <https://doi.org/10.1006/jcis.1996.0030>.
- 1145 [77] Y. Arai, D.L. Sparks, ATR–FTIR Spectroscopic Investigation on Phosphate Adsorption
1146 Mechanisms at the Ferrihydrite–Water Interface, *Journal of Colloid and Interface Science*.
1147 241 (2001) 317–326. <https://doi.org/10.1006/jcis.2001.7773>.
- 1148 [78] E.J. Elzinga, D.L. Sparks, Phosphate adsorption onto hematite: An in situ ATR-FTIR
1149 investigation of the effects of pH and loading level on the mode of phosphate surface
1150 complexation, *Journal of Colloid and Interface Science*. 308 (2007) 53–70.
1151 <https://doi.org/10.1016/j.jcis.2006.12.061>.
- 1152 [79] W. Li, A.-M. Pierre-Louis, K.D. Kwon, J.D. Kubicki, D.R. Strongin, B.L. Phillips,
1153 Molecular level investigations of phosphate sorption on corundum (α -Al₂O₃) by ³¹P solid
1154 state NMR, ATR-FTIR and quantum chemical calculation, *Geochimica et Cosmochimica*
1155 *Acta*. 107 (2013) 252–266. <https://doi.org/10.1016/j.gca.2013.01.007>.
- 1156 [80] R.J. Atkinson, R.L. Parfitt, R.St.C. Smart, Infra-red study of phosphate adsorption on
1157 goethite, *J. Chem. Soc., Faraday Trans. 1*. 70 (1974) 1472.
1158 <https://doi.org/10.1039/f19747001472>.
- 1159 [81] C. Nguyen Trung, G.M. Begun, D.A. Palmer, Aqueous uranium complexes. 2. Raman
1160 spectroscopic study of the complex formation of the dioxouranium(VI) ion with a variety
1161 of inorganic and organic ligands, *Inorg. Chem.* 31 (1992) 5280–5287.
1162 <https://doi.org/10.1021/ic00051a021>.
- 1163 [82] F. Quilès, A. Burneau, Infrared and Raman spectroscopic study of uranyl complexes:
1164 hydroxide and acetate derivatives in aqueous solution, *Vibrational Spectroscopy*. 18 (1998)
1165 61–75. [https://doi.org/10.1016/S0924-2031\(98\)00040-X](https://doi.org/10.1016/S0924-2031(98)00040-X).
- 1166 [83] F. Quilès, C. Nguyen-Trung, C. Carteret, B. Humbert, Hydrolysis of Uranyl(VI) in Acidic
1167 and Basic Aqueous Solutions Using a Noncomplexing Organic Base: A Multivariate
1168 Spectroscopic and Statistical Study, *Inorg. Chem.* 50 (2011) 2811–2823.
1169 <https://doi.org/10.1021/ic101953q>.
- 1170 [84] L. Borgnino, C.E. Giacomelli, M.J. Avena, C.P.D. Pauli, Phosphate adsorbed on Fe(III)
1171 modified montmorillonite: Surface complexation studied by ATR-FTIR spectroscopy,
1172 (2010) 7.
- 1173 [85] K. Nakamoto, *Infrared and Raman Spectra of Inorganic and Coordination Compounds*,
1174 *Handbook of Vibrational Spectroscopy*. (2006) 21.
- 1175 [86] G. Lu, A.J. Haes, T.Z. Forbes, Detection and identification of solids, surfaces, and
1176 solutions of uranium using vibrational spectroscopy, *Coordination Chemistry Reviews*.
1177 374 (2018) 314–344. <https://doi.org/10.1016/j.ccr.2018.07.010>.
- 1178 [87] J. Čejka, A. Muck, To the infrared spectroscopy of natural uranyl phosphates, *Phys Chem*
1179 *Minerals*. 11 (1984) 172–177. <https://doi.org/10.1007/BF00387848>.
- 1180 [88] J.A. Davis, D.B. Kent, CHAPTER 5. SURFACE COMPLEXATION MODELING IN
1181 AQUEOUS GEOCHEMISTRY, in: M.F. Hochella, A.F. White (Eds.), *Mineral-Water*
1182 *Interface Geochemistry*, De Gruyter, 1990: pp. 177–260.
1183 <https://doi.org/10.1515/9781501509131-009>.
- 1184 [89] M.H. Bradbury, B. Baeyens, Sorption modelling on illite. Part II: Actinide sorption and
1185 linear free energy relationships, *Geochimica et Cosmochimica Acta*. 73 (2009) 1004–1013.
1186 <https://doi.org/10.1016/j.gca.2008.11.016>.
- 1187 [90] I. Jeon, K. Nam, Change in the site density and surface acidity of clay minerals by acid or
1188 alkali spills and its effect on pH buffering capacity, *Sci Rep.* 9 (2019) 9878.
1189 <https://doi.org/10.1038/s41598-019-46175-y>.
- 1190 [91] V. Pekárek, V. Veselý, A study on uranyl phosphates—II sorption properties of some 1-
1191 to 4-valent cations on uranyl hydrogen phosphate heated to various temperatures, *Journal*

1192 of Inorganic and Nuclear Chemistry. 27 (1965) 1151–1158. <https://doi.org/10.1016/0022->
1193 1902(65)80427-4.

1194 [92] V.E. Jackson, K.E. Gutowski, D.A. Dixon, Density Functional Theory Study of the
1195 Complexation of the Uranyl Dication with Anionic Phosphate Ligands with and without
1196 Water Molecules, *J. Phys. Chem. A.* 117 (2013) 8939–8957.
1197 <https://doi.org/10.1021/jp405470k>.

1198 [93] M. Stockmann, K. Fritsch, F. Bok, M.M. Fernandes, B. Baeyens, R. Steudtner, K. Müller,
1199 C. Nebelung, V. Brendler, T. Stumpf, K. Schmeide, New insights into U(VI) sorption onto
1200 montmorillonite from batch sorption and spectroscopic studies at increased ionic strength,
1201 *Science of The Total Environment.* 806 (2022) 150653.
1202 <https://doi.org/10.1016/j.scitotenv.2021.150653>.

1203 [94] C. Tournassat, E. Ferrage, C. Poinsignon, L. Charlet, The titration of clay minerals,
1204 *Journal of Colloid and Interface Science.* 273 (2004) 234–246.
1205 <https://doi.org/10.1016/j.jcis.2003.11.022>.

1206 [95] R. Dahn, B. Baeyens, M.H. Bradbury, Uptake mechanisms of U(6) by illite as determined
1207 by X-ray absorption spectroscopy, Organisation for Economic Co-Operation and
1208 Development - Nuclear Energy Agency, Nuclear Energy Agency of the OECD (NEA),
1209 2007.

1210 [96] M. Del Nero, C. Galindo, R. Barillon, E. Halter, B. Madé, Surface reactivity of α -Al₂O₃
1211 and mechanisms of phosphate sorption: In situ ATR-FTIR spectroscopy and ζ potential
1212 studies, *Journal of Colloid and Interface Science.* 342 (2010) 437–444.
1213 <https://doi.org/10.1016/j.jcis.2009.10.057>.

1214 [97] R.L. Frost, An infrared and Raman spectroscopic study of the uranyl micas,
1215 *Spectrochimica Acta Part A: Molecular and Biomolecular Spectroscopy.* 60 (2004) 1469–
1216 1480. <https://doi.org/10.1016/j.saa.2003.08.013>.

1217